Theor Chem Acc (2010) 127:237–257
DOI 10.1007/s00214-010-0758-y

REGULAR ARTICLE

Toward a physical understanding of electron-sharing two-center bonds. II. Pseudo-potential based analysis of diatomic molecules

T. Bitter · S. G. Wang · K. Ruedenberg · W. H. E. Schwarz

Received: 7 December 2009 / Accepted: 13 April 2010 / Published online: 21 May 2010

Abstract A dozen homo- and heteropolar bonds in a series of diatomic molecules are analyzed by an energy partitioning based on the concepts developed in part I of this series (J Comput Chem 28:411–422, 2007). The different bond types are characterized by various physical contributions to the bond energy, namely classical potential interaction, quantum–mechanical orbital interference, and bond stabilizations by atomic configurational promotion, radial deformation, and angular polarization. The effects of the atomic cores are accounted for by means of pseudo-potential operators. Different atomic cores cause specific bond differences. The various bonding mechanisms can be characterized by several parameters. They describe the quantum–mechanical reduction in the 'electronic kinetic energy pressure' due to delocalization (sharing interference) and the increase in the 'molecular potential energy pull' due to overlap of atomic electron densities with adjacent atoms in the molecule. In addition, there are one- and two-electron relaxations whose distinctive features depend on the nature of the cores.

Keywords Bond energy analysis · Bond types · Covalence · Diatomics · Effective core potentials · Polar bond · Pseudo-potentials

1 Introduction

Chemistry as a modern, empirically based science began toward the end of the eighteenth century with the identification of the first few dozen elements. During the next half century, more elements were found, the atomistic structure of matter was recognized, as were the electropolar bond and the homopolar bond. Since then, further types of interatomic linkages were identified, such as the coordinative, metallic, mesomeric, multicenter, van der Waals, hydrogen and metallophilic ones. Present-day chemists speak of primary bonds when bond energies are significantly above 100 (up to 1,000) kJ/mol, whereas the wide variety of interactions that yield stabilizations of significantly less than 100 kJ/mol (down to a few kJ/mol, in particular between closed shell systems) are usually termed secondary bonding in a somewhat vague manner [1, 2].

From the modern theoretical point of view, chemically bonded molecules are characterized by pronounced local minima on potential energy surfaces[1] that satisfy the following criteria. These criteria guarantee the existence of a

Dedicated to the memory of Professor Jürgen Hinze and published as part of the Hinze Memorial Issue.

T. Bitter · S. G. Wang · W. H. E. Schwarz (✉)
Theoretical Chemistry, Fachbereich 8,
University of Siegen, 57068 Siegen, Germany
e-mail: schwarz@chemie.uni-siegen.de

T. Bitter
Ernst Klett-Verlag, Redaktion Chemie, Rotebühlstr. 77,
70178 Stuttgart, Germany

S. G. Wang · W. H. E. Schwarz
Theoretical Chemistry, School of Chemistry,
Shanghai Jiao Tong University, 200240 Shanghai, China

K. Ruedenberg · W. H. E. Schwarz
Department of Chemistry & Ames Laboratory USDOE,
Iowa State University, Ames, IA 50011, USA

[1] Since only small (diatomic) molecules in their electronic ground states at equilibrium conformations are considered in the present study, the presumption of the Born–Oppenheimer separation represents no significant restriction.

chemical bond as defined in the IUPAC Compendium of Chemical Terminology [3, 4].

(i) The energy $E(R_e)$ at the equilibrium geometry R_e is significantly lower than that at somewhat larger distances of the molecular fragments.[2]

(ii) The equilibrium internuclear distance, where $\partial E(R)/\partial R|_{Re}$ vanishes, is significantly shorter than the sum of common atomic van der Waals radii.

(iii) There must be a significant stretching force constant, i.e., curvature $\partial^2 E(R)/\partial R^2|_{Re}$.

The aim of the present investigation is a *quantum–chemical* assessment of the various bonding modes. From this perspective, different types of bonding can be distinguished according to whether the origin of molecule formation can be traced back to changes in the one-electron kinetic energy or in the one-electron potential energy or in the two-electron potential energy. This analysis has been proposed and discussed in some detail in part I of our work [5] and has led to the following conclusions.

(a) *Changes in the kinetic energy functional that result when electrons are shared between atoms* constitute the essential origin of *covalent bonding*. It may be of the homopolar two-center type, of the coordinative or dative type, of the "mesomeric" many-center type as well as of the metallic type. All of such bonds can be described by polycentrically localized molecular orbitals. That electron sharing in fact impacts the quantum–mechanical kinetic energy behavior was first recognized by Hellmann in the 1930s [6–10] and then, e.g., by Peierls [11] and Döring [12] in the 1950s. It was fully elucidated by Ruedenberg since the 1960s [13–16] and subsequently further developed by Kutzelnigg [17–20] and Goddard [21] since the 1970s. It was then also espoused by Fukui [22] and by Mulliken [23]. An updated exposition of the principle was recently given by Ruedenberg and Schmidt [24]. Lewis' conception [25] of a *shared* electron pair as a bonding model, created a decade before the advent of wave mechanics, attests to the power of chemical intuition.

(b) *Changes in the electrostatic attractions between the electron density and the nuclei resulting from interatomic charge transfers toward the more electronegative partners or from extensive charge density overlap* give rise to various kinds of *hetero- and homopolar bonding*. The heteropolar bonding model was already proposed by Kossel [26] before the advent of wave mechanics.[3] In this context, we note that conventional textbooks tend to overemphasize, with respect to all bonds, the importance of electrostatic interactions at the expense of quantum–mechanical kinetic effects.[4]

(c) *Changes in the electron–electron repulsion energy contribute to bonding via energy decreases due to electron correlation* (of the Fermi and Coulomb type). The latter are of two kinds: "Static" correlations, notably "left–right correlations," and "angular correlations around the bond axis," which are accounted for in various valence-bond approaches or by multi-configuration wavefunctions, both based on molecule-adapted optimized minimal basis sets. And the more involved correlations between the motions of the electrons, the "dynamic" correlations. Their binding contributions are due to the increase in the ways electrons can dodge each other, and thereby lower the energy when a molecule is formed. This effect is present in all covalent and polar bonds and can be substantial. It contributes for instance more than 50% to the bond in F_2 [27–29], and it is the sole cause for the bond in Be_2 [30]. It also generates, of course, the long-range dispersion attractions.

In different systems, the three types of bonding contributions (a) to (c) are present to different degrees, and the objective of the present study is to elucidate how this mix can differ in various situations. To this end, we shall discuss a number of exemplifying diatomic molecules. Many of the quantitative data are taken from Ref. [31, 32].

The subsequent exposition proceeds as follows. In Sect. 2, basic concepts on which our analysis is based are outlined. In Sect. 3, we discuss the essential role that electron sharing plays in the formation of a covalent bond by revisiting the accurately analyzed molecules H_2^+ and H_2, where core and cooperating valence electrons are both absent. From this analysis, we deduce a more general parameterized model. In Sect. 4, the effect of atomic cores on bonding will then be discussed by an examination of the molecules Li_2^+ and Li_2. Since the valence shells of the alkali metal atoms are special in that their energetic valence AO sequence is $ns^u < np^v \ll (n-1)d^0$, the subsequent Sect. 5 deals with bonds between atoms whose valence orbitals form the more common sequence $[(n-1)d^{10}] < ns^u < np^v$ [33, 34] with spatially more compact and energetically more bonded valence shells. Here, we discuss on the one hand the molecules Au_2^+ and Au_2, which have big atomic cores, viz. a closed d^{10}-shell, and more strongly bound valence *s*-AOs. On the other hand, we examine typical cases with small atomic cores ('E_2 molecules'). In extension of these sections, heteropolar bonds are considered in Sect. 6, viz. LiH^+ and LiH. Bonds involving π-orbitals (BH, B_2, N_2) are taken up in Sect. 7. (Some of the details in Sects. 5–7, or even 3–7,

[2] This definition, in agreement with the IUPAC bond-definition, comprises stable *and* metastable compounds, where the energy eventually decreases at larger separations. Extreme examples are strained endohedral cage compounds such as He@adamantane with nonbonded repulsions between the 'bonded' fragments [110, 111].

[3] Electropolar bonding ideas go back 200 years, e.g., to Berzelius (~1815) and von Helmholtz (~1875) [112].

[4] This 'textbook wisdom' is reflected, for instance, in the Wikipedia [http://en.wikipedia.org/Chemical_bond].

may be skipped in a first cursory reading.) The insights gained by the analyses regarding similarities and differences of bonding mechanisms are then synthesized in a general classification scheme in Sect. 8.

Unless specified otherwise, we give energies in eV ($\approx$1/27.2114 hartree $\approx$23.0605 kcal/mol $\approx$96.4853 kJ/mol) and lengths in atomic units (1 bohr $\approx$52.9177 pm).

2 Elements of the present bonding analysis

2.1 General premises

Chemical bonds result from *differences in quantum–mechanical electronic ground state energies for different geometric arrangements* of a given set of atoms. Understanding the origin of binding is therefore contingent upon understanding (i) the change of the wavefunction between the bonded molecule and unbound reference fragments and (ii) the effect of wavefunction shapes on the magnitudes of ground state energies. A rigorous universal basis for such an understanding is provided by the variation principle. It shows that the ground state wavefunction is the one that optimally exploits the available electrostatically attractive energy regions while at the same time keeping the concomitant positive kinetic energy increases as small as possible.

Various aspects of this *variational competition between the kinetic and the potential energy as a basis for physical understanding* have been elaborated in detail in Refs. [5–24]. In particular, it has been explicitly demonstrated how answers to the questions *why?* and *how?* can be found by this approach, *provided one compares values of the energy functional for judiciously chosen nonstationary, though physical trial wavefunctions on the variational path from the chosen separated fragments to the molecular energy minimum*. It was also shown that such questions cannot be answered nor elucidated if one limits oneself strictly to examine the wavefunction (or even only the density distribution) of the *actual molecular* stationary ground states.

The sole investigation of *molecular* wavefunctions or densities cannot answer the question of the bond origin. Bond energies are energy *differences,* and this implies the comparison of a molecule with a nonbonded reference state. The use of the aforementioned *variational reasoning* to explain, say, that the system of atoms A and B has a lower energy at its bonded molecular equilibrium distance than at larger separation, therefore requires an additional piece of reasoning. Namely: One has to formulate *an initial trial wavefunction for the more stable system (in this case the molecule) that can be simply related to the less stable system (the chosen reference system, e.g., the separated atoms)*.

To this end, we shall define an intermediate construct of *overlaid atoms* at the molecular separation. In a first step, the energy difference between the separate atoms and this intermediate molecular trial wavefunction is deduced from physical considerations. In a second step, the energy lowering that occurs when this intermediate molecular trial wavefunction relaxes into the actual molecular wavefunction can be understood on the basis of variational reasoning. A similar philosophy had been implemented by Morokuma, Ziegler, Baerends (MZB), and others [35–39]. In order to gain further physical insights, each of the two steps will typically be resolved into substeps, whose energy changes are conceptually evident. In this manner, the total binding energy ends up as the sum of a number of interpretable energy contributions.

The overlay of the atoms will be resolved first into two substeps. In the first, *atomic densities* will be overlaid, undeformed in the spirit of *classical* lowest order perturbation theory (PT). While this seems simple, it can nonetheless result in chemically surprising energy contributions [40]. Since the wavefunction amplitudes are, however, the real entities in the quantum world [41, 42], the second substep consists of overlaying the undeformed *atomic wavefunctions* in the spirit of *quantum*–mechanical lowest order PT. This leads to quantum–mechanical interference and the implications of the Pauli principle. The energy change of these two substeps of the overlay of the free atoms is called the steric energy in the MZB approach.

Concerning possible substeps of the variational relaxation from the overlaid atoms to the molecular energy minimum, we follow these guidelines: If possible, large dominant contributions should have the same sign because cancellations of large contributions of opposite sign do not yield simple convincing qualitative bonding pictures. A given bond energy can be partitioned into a very large number of possible energy terms (see e.g., Ref. [35]). We try to combine them so as to yield a few meaningful quantities characteristic of the given bond. That is, cancellations between many (even important) possible energy contributions should be hidden so that bonds will be characterized by (i) the bond-specific partitioning as well as by (ii) the individual values of those energy pieces. Such a 'self-organizing' partitioning procedure should extract the overall phenomenon that is specific for a given bond rather then bury it under a wealth of data of a too detailed breakdown. It should put in evidence the bonding mechanism that is essential to the given bond. In particular, the kinetic aspects should not be lost by the sole consideration of electrostatic or density terms, as e.g., in Refs. [43, 49].

Manifestly, there exists not just one method for describing and explaining the chemical bonding phenomena. Various approaches highlight various, complementary aspects. For instance, one may analyze wavefunctions or density matrices, or at a lower level of information contents, the electron density distribution [44, 45], hoping that

chemically sufficiently accurate relations between charge density and both, the kinetic energy [46, 47] and also the two-electron Coulomb energy can be found, eventually. Or one may discuss the low energy of bonded molecules, or the vanishing forces [48] in bonded and in separated, nonbonded structures.[5] One may also define the bonded atoms constituting the molecules as optimally transferable overlapping entities or as sharply separated entities strongly depending on the bonded situation [49]. And one may think of molecules as consisting of deformed atoms or of atomic *and* bond contributions [50, 51].

2.2 Pseudo-potential treatment of atomic cores

A distinctive feature of the present analysis is the treatment of the chemically inactive atomic cores by the pseudo-potential method. Pseudo-potentials or effective core potentials simulate the complex quantum–mechanical actions of the inner occupied shells, viz. nuclear shielding, core polarization, and closed shell Pauli repulsion, in a manner that is easier to visualize. In the present context, this approach has three benefits.

(i) The quantum–mechanical influence of occupied core shells on the behavior of valence electrons is intricate. In quantum–chemical ab initio approaches, the valence orbitals are usually orthogonalized to the occupied core orbitals. This causes an oscillatory behavior of the valence orbitals in the core region, which allows only a low overall probability for the penetration of the valence orbitals into the core region (typically $\sim 10\%$). Nonetheless, the inner core wiggles of the valence orbitals cause comparatively large, partially compensating contributions to the electronic kinetic and potential energies [52] and to the electrostatic forces [53]. These effects are replaced by a conceptual Pauli-repulsive pseudo-potential, which keeps the valence shells out of the atomic cores without introducing tedious core wiggles, while simultaneously yielding the correct total energy.

(ii) While the total valence shell energies E_v are much smaller than the core energies, the kinetic part T_v and the potential part V_v of the valence energy are much larger in magnitude than E_v [52]. The pseudo-potential method accomplishes the separation of these large, but mutually canceling, core-related contributions, say T_v^* and V_v^*, from the proper valence contributions, which are then the pseudo-potential energies T_{ps} and V_{ps}. This corresponds to the resolutions

$$T_{total} - T_{core} = T_v = T_v^* + T_{ps},$$
$$V_{total} - V_{core} = V_v = V_v^* + V_{ps}, \quad (1)$$
$$E_{total} - E_{core} = E_v = T_v + V_v = T_{ps} + V_{ps}, \text{ with}$$
$$T_{ps} \ll T_v^*, |V_{ps}| \ll |V_v^*|, T_v^* + V_v^* = 0. \quad (2)$$

The implication is that those Pauli repulsions that are caused by *kinetic* energy terms due to orthogonalization to the core are replaced by certain repulsive terms in the *potential* energy. The valence solutions of Schrödinger equations with pseudo-potentials are wavefunctions that are significantly changed in the core region and, as a result, they do not satisfy the virial theorem in the form $-V/T = 2$ that holds for the total energies.[6] Rather, one finds that

$$-V_{ps}/T_{ps} = 2 + \varepsilon \quad \text{with } 0 < \varepsilon < \alpha, \quad (3)$$

where α is of the order of 1, typically between 0 and 2. Concomitantly, one finds that T_v and V_v do not satisfy the simple Coulombic virial theorem either. From Eq. (3) follows

$$-E_v/T_{ps} = -1 - V_{ps}/T_{ps} = 1 + \varepsilon, \quad (4)$$

and hence

$$-V_v/T_v = 1 - E_v/T_v = 1 - (E_v/T_{ps}) \times (T_{ps}/T_v) \quad (5)$$
$$= 1 + \delta \quad \text{with} \quad 0 < \delta \ll 1, \quad (6)$$

since $T_{ps} \ll T_v$, as mentioned above.

(iii) The variation of molecular properties and bond energies down the periodic table (e.g., from Li to Cs or Au or from Cr to U or Sg) and the differences between the *s–p* and *d–f* groups (Cs/Au or U/Sg) are easily rationalized by differences in the pseudo-potential shapes. For instance, Kutzelnigg has traced back the difference between second and third row chemistry to relative differences in the atomic *s*- and *p*-valence orbitals, which can be further rationalized by the differences in the *s*- and *p*-pseudo-potentials [54–59]. The pronounced tendency in the (middle of the) second row of the periodic table to form bonds with *s–p* valence hybrids is related to the

[5] Not *every* putative explanation is valid, however. This observation notably applies to the following often advanced propositions: (a) that covalent bonds essentially come about because atomic orbital overlap accumulates electronic charge between the atoms, which is then electrostatically attracted by two nuclei instead of only one, (b) that the kinetic energy changes only collaterally, and (c) that these inferences are implied by the virial theorem. None of these and related conjectures (e.g. [43, 74, 75, 103–107]) and various textbooks) have ever been buttressed by explicit calculations. Rather, detailed quantitative studies [13–24] have shown that the essential element of *covalent* bonding is the reduction of the *kinetic* energy that results from the delocalization inherent in interatomic electron sharing. This is also in accordance with the fact that it is the treatment of the *kinetic* energy that distinguishes quantum mechanics from classical mechanics. On the other hand, dominant *potential* contributions to the binding energy and, even more, to the attractive force [53] arise from regions near to the nuclei.

[6] The virial ratio $-V/T$ is >2 for real extended non-point nuclei, and also in density functional approaches, though the deviations from 2 are small. For quasi-relativistic perturbation calculations, $-V/T$ is slightly below 2.

similar radial extension of the 2*s* and 2*p* AOs, while *n*p AOs are comparably more extended than the *n*s AOs for $n \geq 3$. The qualitative explanation is that 2*s* 'feels' the Pauli-repulsive pseudo-force of the $1s^2$ shell, while 2*p* 'feels' the centrifugal pseudo-force $+l(l+1)/2r^3$, which turn out to be of similar magnitudes. However, *n*s feels the Pauli repulsion of $(n-1)s^2$, while *n*p feels more repulsion, viz. *both* the $(n-1)p^6$ Pauli and the $l=1$ centrifugal pseudo-forces.

(iv) Since, in all-electron calculations, the virial theorem applies to the *total* energy, it is to be expected that small changes in the large core energies will have a marked impact on the preservation of the virial ratio $-V/T$ upon bond formation, even though the core changes have only a small effect on the total binding energy. Bonding analyses that differ in the treatment of cores, say by "freezing" them [39], or by including them in pseudo-potentials, will therefore differ in the assessment of changes in the ratio between *T* and *V*, even if they agree in the overall bonding picture.

3 Covalent bonding through electron sharing

3.1 Variational competition

The basic question of bond formation is why is the energy, the sum of a kinetic and a potential part, lower at the molecular equilibrium distance than at larger separation? As already mentioned at the beginning of Sect. 2.1, there exists a *variational competition* between two tendencies: the potential energy can lower its value by pulling the wavefunction closer toward the nuclei, while the quantum kinetic energy can lower its value by making the wavefunction broader. By virtue of the variation principle, the actual ground state wavefunction is the one that offers the *optimal compromise between the localizing potential pull and the delocalizing kinetic pressure*. Hence, it must be that, at the equilibrium distance, either the kinetic pressure is weaker or the potential pull is stronger than at larger separation (or both apply). We shall see that, *for the case of* H_2^+ *and* H_2, *it is the kinetic pressure that is weaker at the equilibrium position and that this softening is a direct consequence of electron sharing.*

The simplest illustration of the variational competition is furnished by the hydrogen atom with trial orbital

$$\phi = N\ \exp(-r/\alpha), \quad N = (\alpha^3\pi)^{-1/2}. \tag{7}$$

The explicit dependences of the *T* and *V* values on α are (in atomic units)

$$T(\alpha) = +\frac{1}{2}\int \mathrm{d}r \cdot |\nabla\phi(r)|^2 = 1/(2\alpha^2), \tag{8}$$

$$V(\alpha) = -\int \mathrm{d}r \cdot r^{-1} \cdot |\phi(r)|^2 = -1/\alpha, \tag{9}$$

with optimum value $\alpha = 1$ for the minimum of their sum. This yields the exact 1*s* atomic orbital of the hydrogen atom. The variational parameter α is a measure of the size of the orbital, *viz.* $\langle\phi|r|\phi\rangle = 1.5\alpha$. Because of the normalization of ϕ, its gradient will become steeper when, for increasing α, ϕ is squeezed into a smaller space. One can also argue in terms of the uncertainty principle[7]: for orbital (7), the spatial uncertainty Δr is essentially α and the momentum uncertainty is then $\Delta p = |\,p\,| \approx \hbar/\Delta r$, hence the lowest value for $T = p^2/(2\ \mathrm{m})$ is of order $\hbar^2/(2\ \mathrm{m}\alpha^2)$, i.e., $1/(2\alpha^2)$ in atomic units. It is a general and typical quantum–mechanical phenomenon that *delocalization of an electron cloud lowers its kinetic energy integral* (provided that no additional nodes are introduced).

The three *dashed* plots in Fig. 1 exhibit the kinetic energy integral $T(\alpha)$, the potential integral $V(\alpha)$, and the total energy integral $E(\alpha) = T(\alpha) + V(\alpha)$ as functions of the orbital size α. While $V(\alpha)$ decreases when the orbital shrinks toward the nucleus, the opposite is the case for $T(\alpha)$, which exhibits the outward kinetic pressure[13]. The optimal compromise is the minimum on the curve for $E(\alpha)$, whose position is marked by an asterisk on the three curves.

3.2 The one-electron bond without core: H_2^+ (Table 1)

In its purest form, the bond-forming power of *electron sharing* is exhibited in H_2^+ and H_2. It is true that these molecules are somewhat atypical inasmuch as they have no chemically inactive cores, which has been noted repeatedly [17, 49, 60–62] even before the advent of quantum mechanics [63]. Nonetheless, their analysis yields basic insights into the quantum–mechanical mechanism of *covalent* bonds in general. Historically, they were the first to be described successfully by quantum theory in the late 1920s [64–73] and they were also the first where the origin of binding was understood in the early 1960s [13–16]. We here follow the discussions of Ruedenberg [13–16], Kutzelnigg [17–20], Goddard [21], Fukui [22], and Mulliken [23].

3.2.1 *Physical origin of bonding in* H_2^+

We consider the hydrogen molecule ion at its equilibrium distance of 2 bohr. The normalized wavefunction of $(H_A - H_B)^+$ can be written as

$$\psi = (\psi_A + \psi_B)/\sqrt{[2(1+S)]}, \quad S = \langle\psi_A|\psi_B\rangle, \tag{10}$$

[7] For common one-particle states, the relation $\Delta r \cdot \Delta p \approx n\hbar$ holds approximately, where *n* is the principal quantum number.

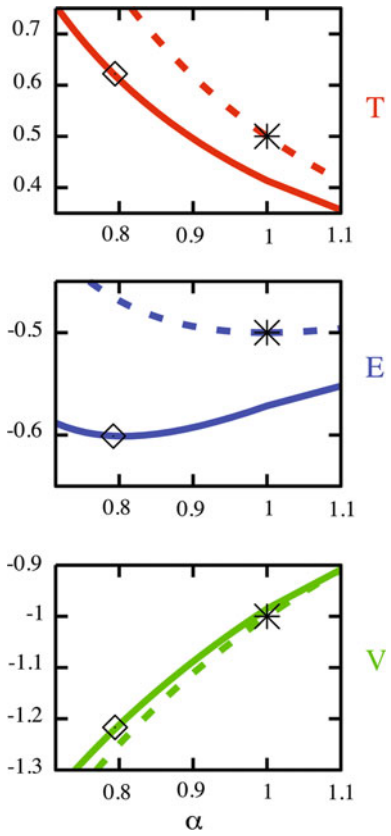

Fig. 1 Competition between kinetic energy T (*upper panel*) and potential energy V (*lower panel*) in determining the variational minimum of the total energy E (*center panel*) in the H atom (*dashed lines*) and in the H_2^+ ion at $R = 2$ bohr (*solid lines*) [10–13, 20]. Abscissa: orbital size parameter α (in bohr), ordinate: energies (in Hartree; note: the energy scale of the center panel is expanded). The markers (*asterisk* for H and *open diamond* for H_2^+) indicate the positions of the respective total energy minima. The *reduction* in the T-function from *dashed* to *solid*, with the V-function remaining nearly unchanged, entails a lower E function for the molecule with a minimum E that has a *higher* T-value

$$\psi_A = \phi_A \times (1 + \gamma_A), \quad \psi_B = \phi_B \times (1 + \gamma_B). \tag{11}$$

$\phi_{A,B}(r;\alpha)$ is the atomic orbital (7) at centers A, B, respectively. For $R = 2$ bohr, the *optimal* atomic orbital size is $\alpha = 0.7903$, which represents a *shrinking of the molecular orbital toward both nuclei A and B*. The functions γ describe angular "polarizations," which vary from zero for the free atoms ($\alpha = 1$) to small values in the molecule.[8] The kinetic, potential, and total energy integrals, calculated from the orbital (10) as functions of the orbital size parameter α, are exhibited by the *solid* curves in Fig. 1 [24].

These curves are quite similar in shape for atom and molecule, which shows that the variational competition between potential pull and kinetic pressure determines the optimal compromise for the ground state orbitals of atoms and molecules in a similar manner. However, two differences between the H atom and the H_2^+ molecule are apparent: (i) The kinetic energy curve $T(\alpha)$ of H_2^+ runs significantly lower than that of H for all α. (ii) The potential energy curve $V(\alpha)$ of H_2^+ runs higher, but only weakly. That is, the intrinsic kinetic pressure of the electron is weakened in the molecule while the potential pull by the nuclei has not increased. *Thus, the bicentric delocalization of the electron softens the kinetic energy pressure and, as a consequence, the nuclear potential attraction is able to attach the electronic cloud more tightly to the nuclei in the molecule, which lowers the total energy.*

A peculiar aspect is that the kinetic energy of H_2^+ at *its* variational minimum is *higher* than the kinetic energy of H at *its* variational minimum. This is a consequence of the different dependences of the kinetic energy pressure and the nuclear pull on the orbital size parameter, *viz.* α^{-2} and α^{-1}, respectively, which entails the *virial theorem* $E = -T = V/2$. This (nonrelativistically rigorous) theorem is valid for atoms and for molecules at equilibrium geometries. It implies that, upon bond formation, the kinetic energy will *always* increase and the potential energy will always decrease regardless of the type of bonding.

3.2.2 Bonding as interaction between atoms

The formation of the molecular orbital ψ as a *superposition of deformed atomic orbitals*, as given by Eqs. (10, 11), is the mathematical expression of the chemical concept of *electron sharing* between atoms. It allows a more detailed analysis by examining the variational process in several steps. The numerical energy values are listed in Table 1.

(i) The first substep is to place a proton B near a hydrogen atom A at the equilibrium distance of H_2^+ ($\sim$2 bohr) without changing the 1*s* electron orbital on A. The resulting energy change due to this 'sudden' approximation is the *quasiclassical electrostatic interaction energy* (ΔC),

$$V(\Delta C) = 1/R_{AB} - \langle 1s_A|1/r_B|1s_A\rangle, \tag{12}$$

with value $V = +0.752$ eV. It is repulsive ("antibonding") because the proton B lies somewhat inside the electron cloud around atom A, which therefore does not completely shield B from the repulsion by nucleus A.

(ii) The second substep is to form the *shared* wavefunction of the undeformed atomic 1s orbitals, however, with unmodified $\alpha_A = \alpha_B = 1$ and $\gamma_A = \gamma_B = 0$ in Eqs. (10, 11). This sharing step is found to increase the potential energy further by $V(\Delta I) = +0.882$ eV. This antibonding effect can be understood by expressing the density of the wavefunction as

[8] The major non-sphericity around each nucleus is already brought about by the superposition of ϕ_A and ϕ_B [113].

Table 1 Energy decomposition (in eV) of H_2^+ at $R = 2$ au $\approx R_e$

H_2^+	$T_\parallel$	$T_\perp$	T	V_{nn}	V_{ne}	V	E
Separated atoms	+4.54	+4.54	+13.61	–	−27.21	−27.21	−13.61
Molecule	+3.80	+6.30	+16.40	+13.61	−46.40	−32.80	−16.40
Bond energy ($\Delta E = \Delta O + \Delta D$)	**−0.74**	**+1.76**	**+2.79**	+13.61	−19.19	**−5.59**	**−2.79**
Quasiclassical interaction (ΔC)	–	–	–	+13.61	−12.86	+0.75	+0.75
Quantum interference (ΔI)	−2.07	−0.51	−3.09	–	+0.88	+0.88	−2.21
Total overlay effect ($\Delta O = \Delta C + \Delta I$)	**−2.07**	**−0.51**	**−3.09**	+13.61	−11.98	**+1.63**	**−1.46**
Radial orbital relaxation (ΔR)	+1.22	+2.13	+5.48	–	−6.50	−6.50	−1.02
Angular orbital relaxation (ΔA)	+0.11	+0.15	+0.41	–	−0.72	−0.72	−0.31
Total atomic deformation ($\Delta D = \Delta R + \Delta A$)	**+1.33**	**+2.28**	**+5.89**	–	−7.22	**−7.22**	**−1.33**

$T_\parallel$ = bond-parallel component of kinetic energy of valence electron(s); $T_\perp$ = one of the two bond-vertical components; $T = T_\parallel + 2T_\perp$ = total electronic kinetic energy; V_{nn} or V_{cc} = nuclear-nuclear or core-core repulsion energy; V_{ne} or V_{ce} = nuclear-electron Coulomb or core-electron effective (pseudo-potential) attraction energy; V_{ee} = electron–electron repulsion energy; $V = V_{nn} + V_{ne} + V_{ee}$ = total potential energy; $E = T + V$ = total energy. ΔE = total bond energy BE; ΔO = overlay energy of undeformed atoms; ΔD = deformation energy of the atoms in the molecule; ΔC = quasiclassical electrostatic interaction energy; ΔI = quantum interference energy; ΔR = radial orbital relaxation energy; ΔA = angular orbital relaxation energy; ΔP = polar charge transfer energy.

* *In subsequent tables*: the asterisk indicates bond energy values that are empirically corrected for valence electron correlation, see text at the end of Sect. 3. For units, see end of Sect. 1. Bold values represent the differences or sums of the respective contributions in the preceding lines

$$\rho = \psi^2 = \rho_o + \rho(\Delta I) \quad \text{with} \tag{13}$$

$$\rho_o = \frac{1}{2}(\psi_A^2 + \psi_B^2), \qquad \rho(\Delta I) = (\psi_A \cdot \psi_B - S \times \rho_o)/(1 + S). \tag{14}$$

The term ρ_o represents the quasiclassical density averaging of the undeformed atoms. The difference $\rho(\Delta I) = \rho - \rho_o$ is due to the quantum–mechanical amplitude superposition and is therefore called the *quantum interference* term (ΔI). Since ρ and ρ_o are both normalized to unity, this interference term represents a *charge shift*. Fig. 2 shows that it moves charge *from the regions near the nuclei with low potential into the bond region of higher potential*. Therefore, the *'bond charge accumulation' raises* the nuclear-electronic attraction energy.

The major effect of electron sharing is, however, the substantial drop in the kinetic energy, namely by $T(\Delta I) = -3.094$ eV for the delocalized electron. This was already realized by Hellmann in 1933 [6]. Ruedenberg [13–16] and Kutzelnigg [17–20] have discussed it as kinetic *interference stabilization*; Goddard [21] has related it to the contragradience of the superposed atomic orbitals. The zeroth-order overlay wavefunction thus yields a total energy lowering of $E(\Delta O) = -3.094 + 0.752 + 0.882$ eV $= -1.460$ eV, which is about half of the actual binding energy of −2.793 eV. The lowering is due to the dominant kinetic energy lowering notwithstanding an increase in the potential energy at this stage. Unfortunately, many textbooks still teach the invalid conjecture (going back, it seems, to Ref. [74, 75], see footnote[5]) that charge accumulation in the bond *lowers the potential energy* (and is *therefore* the cause of binding),

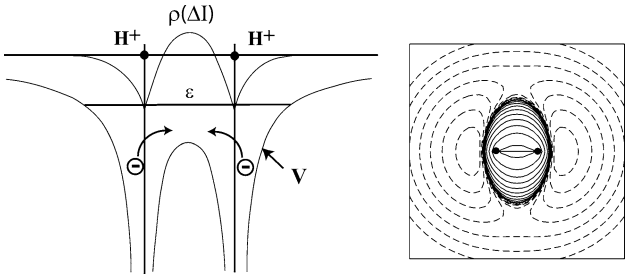

Fig. 2 *Left*: Energy ε and potential function V along the internuclear axis of H_2^+ for a valence electron in the field of two protons H^+ at equilibrium distance. *On top*: sharing interference density redistribution $\rho(\Delta I)$. Bond charge concentration raises the potential energy. *Right*: Optimized difference density of ($H_2^+ - 2H^{1/2+}$), contour line values are $\pm 0.000675 \cdot 2^n$ e/Å^3, $n = 0, 1, 2, \ldots$. *Dashed lines* are negative

failing to take into account the concomitant charge depletion near the nuclei.

(iii) The final step in our analysis is the examination of the energy changes, when the molecular wavefunction relaxes variationally to the "final" wavefunction. From Eqs. (10, 11) it is apparent that two kinds of orbital deformations occur: radial deformations (ΔR), *viz.* orbital shrinkage (from atomic $\alpha = 1$ to molecular $\alpha = 0.7903$), and angular deformation (ΔA), *viz.* orbital polarization. In the H_2^+ molecule, the former is by far more important ($E(\Delta R) = 77\%$ of $E(\Delta D)$). This orbital deformation changes the total binding energy by $E(\Delta D) = -1.33$ eV, lowering it to the final molecular value of $E(H_2^+) = -2.79$ eV. The kinetic and potential components change by much greater amounts (Table 1).

Insight into the reason for these changes is offered by the virial ratios $|V|/T$ of the H atom, of the (physical, though not yet energy-minimized and stationary) overlay function of step (ii) and of the variationally minimized wavefunction, namely

$$\begin{aligned} &\text{separated } H + H^+ \text{ atoms } |V|/T = 2, \\ &H_2^+ \text{overlay function of step } (ii) |V|/T = 2.433137, \\ &H_2^+ \text{actual final wavefunction } |V|/T = 2. \end{aligned} \tag{15}$$

The value of 2 for the stationary atom and molecule is known in advance. The higher value of the overlay function is a result of the discussed kinetic energy lowering through electron sharing. The virial ratio >2 indicates that this approximate function is not yet sufficiently compact. Hence, the variational minimization will shrink the orbital so as to increase T and lower V until the virial ratio is lowered to the value 2.

3.3 A model for the variational competition

In the relevant range of α covered in Fig. 1, the variational kinetic and potential *molecular* energy curves can be simply related to the *atomic* curves, namely: The atomic functions $1/(2\alpha^2)$ and $-1/\alpha$ of Eqs. (8, 9) are essentially multiplied by constant factors. The actual kinetic and potential energy functions of H_2^+ are in fact quite accurately reproduced by

$$\begin{aligned} T(\alpha) &= (1-\kappa) \times 1/(2\,\alpha^2), \\ V(\alpha) &= (1+\pi/2) \times (-1/\alpha), \end{aligned} \tag{16}$$

where $\kappa = 0.247$ and $\pi = -0.095$. Variational minimization of $E(\alpha)$ using Eq. (16), which will satisfy the virial relation, yields $\alpha = 0.7905$ and a binding energy of -2.787 eV when compared to the exact values $\alpha = 0.7903$ and -2.793 eV.

The parameters κ and π in Eq. (16) may furnish a general model for the kinetic and potential energy effects of atomic orbital interference and electrostatic interaction. The value of κ, which embodies the drop of the kinetic energy pressure due to delocalization, can be understood as follows. In the bond axis direction, the orbital of H_2^+ is about twice as long as one of the superposed atomic orbitals. Hence, Hellmann's [6–10] particle-in-a-box delocalization model would suggest a reduction in the bond-parallel atomic component $T_{\|} = 1/6$ hartree by a *factor* 1/4, which yields a kinetic energy *decrease* by $3/4 \times 1/6 = 1/8$ hartree. With the bond-perpendicular components unchanged, this decrease represents 25% of the total atomic kinetic energy of 1/2 hartree, a reduction corresponding to $\kappa = 0.25$, close to the value 0.247 given above.

The model is of interest, because it can be adapted for characterizing other diatomic molecules with atomic cores. This is accomplished by the following generalization of Eq. (16). For the atoms with cores, we choose the *ansatz*

$$T_{at}(\alpha) = k/(2\,\alpha^2), \quad V_{at}(\alpha) = -Z/(v\,\alpha^v), \tag{17}$$

and for the molecule with atomic cores:

$$\begin{aligned} T_{\mathrm{mol}}(\alpha) &= (1-\kappa) \times k/(2\,\alpha^2), \\ V_{\mathrm{mol}}(\alpha) &= (1+\pi/2) \times [-Z/(v\,\alpha^v)]. \end{aligned} \tag{18}$$

k and $(1-\kappa) \times k$ are the atomic and molecular parameters of kinetic pressure, and Z and $(1+\pi/2) \times Z$ are the respective ones for the potential pull. The parameter v simulates the effect of the pseudo-potential, being more attractive than the Coulomb potential outside the core and less attractive inside the core. One may assume $0 < \kappa < 1$, $-2 < \pi$, and $0 < v < 1$. The resulting optimized atomic orbital-radius parameter is $\alpha_{\mathrm{opt}} = (k/Z)^{1/(2-v)}$, and the virial ratio becomes $-V_{\mathrm{ps}}/T_{\mathrm{ps}} = 2/v = 2 + \varepsilon > 2$ (see Eq. 3).

For the core-free Coulombic case, *viz.* $v = 1$ and $-V/T = 2$, the respective molecular variational minimizations of E with respect to α yield

$$\alpha_{\mathrm{at}} = k/Z, \quad T_{\mathrm{at}} = Z^2/2k, \quad V_{\mathrm{at}} = -Z^2/k \tag{19a}$$

$$\alpha_{\mathrm{mol}} = \alpha_{\mathrm{at}}[(1-(2\kappa+\pi)/(2+\pi)], \tag{19b}$$

$$T_{\mathrm{mol}} = \mu T_{\mathrm{at}}, \quad V_{\mathrm{mol}} = \mu V_{\mathrm{at}}, \quad E_{\mathrm{mol}} = \mu E_{\mathrm{at}}, \tag{20a}$$

$$\mu = 1 + (\kappa+\pi) + (\kappa+\pi/2)^2/(1-\kappa). \tag{20b}$$

For $\pi > -\kappa$, this model yields $E_{\mathrm{mol}} < E_{\mathrm{at}}$ (bonding stabilization) and $\alpha_{\mathrm{mol}} < \alpha_{\mathrm{at}}$ (orbital contraction), as in H_2^+. The four model parameters k, Z, κ, and π can be determined from the atomic and molecular energies.

As in Step (ii) of Sect. 3.2.2 for H_2^+, the virial theorem is, however, not satisfied for the zeroth-order sharing step, i.e., for the approximate energy of the overlay of the superposed undeformed atoms. They have $\alpha_{\mathrm{ov}} = \alpha_{\mathrm{at}} = k/Z$, whence

$$\begin{aligned} T_{\mathrm{ov}} &= (1-\kappa) \times T_{\mathrm{at}}, \quad V_{\mathrm{ov}} = (1+\pi/2) \times V_{\mathrm{at}}, \\ E_{\mathrm{ov}} &= (1+\kappa+\pi) \times E_{\mathrm{at}} \end{aligned} \tag{21}$$

with the virial ratio

$$-V_{\mathrm{ov}}/T_{\mathrm{ov}} = 2 + (2\kappa+\pi)/(1-\kappa). \tag{22}$$

Since $\pi > -\kappa$, this is again larger than 2. From Eqs. (19a–21) follows then

$$T_{\mathrm{mol}} = T_{\mathrm{ov}} + T_{\mathrm{at}} \times \left[2\kappa + \pi + O^2(\kappa,\pi)\right] \quad > T_{\mathrm{ov}}, \tag{23a}$$

$$V_{\mathrm{mol}} = V_{\mathrm{ov}} - T_{\mathrm{at}} \times \left[2\kappa + \pi + 2O^2(\kappa,\pi)\right] < V_{\mathrm{ov}}, \tag{23b}$$

$$E_{\mathrm{mol}} = E_{\mathrm{ov}} - T_{\mathrm{at}} \times O^2(\kappa,\pi) \qquad < \mathrm{E_{ov}}, \tag{23c}$$

where $O^2(\kappa, \pi) = (\kappa + \pi/2)^2/(1-\kappa)$. These equations show that the reduction in the kinetic pressure (approximately $-\mathbf{1}\boldsymbol{\kappa}$) and change of the potential pull (approximately $-\mathbf{1}\boldsymbol{\pi}$) *at the overlay stage* induce a variational decrease in the potential energy, a slightly smaller increase in the kinetic energy, and a much smaller decrease in the

total energy. The origin of binding in this model is thus again due to a reduced kinetic pressure (positive κ parameter) and/or to an increased potential pull. Again, the final kinetic energy change (approximately $+\mathbf{1}\boldsymbol{\kappa} + \mathbf{1}\boldsymbol{\pi}$) and potential energy change (approximately $-\mathbf{2}\boldsymbol{\pi} - \mathbf{2}\boldsymbol{\kappa}$) provide no information regarding the physical mechanism of molecule formation. The extended model (17, 18) for more realistic atoms with cores must be evaluated numerically and will prove helpful in comparing various bond types.

3.4 The two-electron bond without core: H_2 (Table 2)

The covalent bond in H_2 is the result of two electrons being individually shared between two atoms. Basically, it is the cumulative effect of two one-electron bonds as in H_2^+. There are, however, some differences and additional interactions.

3.4.1 Quasiclassical electrostatic interaction

When the outer electrons of one neutral spherical atom penetrate into the electron cloud of another atom, they feel the incompletely shielded nuclear attraction of the latter. Many introductory chemistry courses give the incorrect impression that two neutral atoms with overlapping electron shells repel each other electrostatically, which would yield a positive $V(\Delta C)$. In general there is, however, a *significant* electrostatic attraction with negative $V(\Delta C)$, well known from the Morokuma-Ziegler-Baerends bond energy analyses [35–40, 76]. In the special case of H_2 (Table 2), with few electrons and an exceptionally short internuclear distance, causing comparatively large internuclear repulsion, $V(\Delta C)$ though negative is still small, *viz.* only -0.06 eV (without correlation correction).

3.4.2 Coulomb correlation

Electrons of an interpenetrating classical system would perform dodging Coulomb correlations, and this would lower the potential energy. Correlation density functionals deduce approximate correlation stabilizations from the one-electron density. Here, we will use the following semi-empirical recipe: We add the estimated molecular minus atomic correlation energy (a negative value) with factor $+1$ to $V(\Delta C)$, $V(\Delta I)$, $E(\Delta C)$, $E(\Delta O)$, and ΔE, with factor 2 to $V(\Delta O)$ and $V(\Delta E)$, and with factor -1 to $T(\Delta I)$, $T(\Delta O)$, and $T(\Delta E)$. For the H_2 bond, the correlation energy is -1.12 eV. This gives -1.18 eV for the correlation-corrected $V(\Delta C)$.

3.4.3 Interference and relaxation

These features, qualitatively similar to those in H_2^+, are quantitatively different. The model parameters simulating the values in Eq. (16) are now $\kappa = +0.15$ and $\pi = -0.02$, which yield $\alpha_{mol} = 0.86$. Again, the potential effect is small! The bond formation is dominated by the kinetic effect. Since there are no atomic core shells, the two bonding electrons in H_2 lead to a particularly short bond, even in comparison to H_2^+. The small space in H_2 is less helpful for sharing interference, so that the value of $T(\Delta I)$ in H_2 is not quite twice that in H_2^+. Since the two bonding electrons repel each other, the contraction of the atoms in the molecule is less pronounced and less efficient in H_2 than in H_2^+. The overlay and deformation density changes are shown in Fig. 3 (left).

4 Bonding with atomic core repulsions

4.1 The Bond of Li_2^+ (Table 3)

Pseudo-potential virial ratios are $-V_{ps}/T_{ps} > 2$, for the Li atom ≈ 3.5. The spatial dimensions of Li are larger, and the absolute valence energy values are smaller than for H by factors of 2 to 3. The same holds for the respective molecular values.

Table 2 Energy decomposition (in eV) of H_2 at $R = 1.4$ au $\approx R_e$

H_2	$T_\parallel$	$T_\perp$	T	V_{nn}	V_{ne}	V_{ee}	V	E
Separated atoms	+9.07	+9.07	+27.21	–	−54.43	–	−54.43	−27.21
Molecule	+7.94	+11.45	+31.96*	+19.44	−99.09	+17.97	−63.91*	−31.96*
Bond energy ($\Delta E = \Delta O + \Delta D$)	**−1.13**	**+2.38**	**+4.75***	+19.44	−44.66	+17.97	**−9.49***	**−4.75***
Quasiclassical interaction (ΔC)	–	–	–	+19.44	−33.20	+13.70	−1.18*	−1.18*
Quantum interference (ΔI)	−3.33	−0.83	−3.88*	–	+0.89	+1.70	+1.47*	−2.41
Total overlay effect ($\Delta O = \Delta C + \Delta I$)	**−3.33**	**−0.83**	**−3.88***	+19.44	−32.31	+15.40	**+0.29***	**−3.60***
Radial orbital relaxation (ΔR)	+1.74	+3.37	+8.48	–	−11.84	+2.37	−9.47	−0.99
Angular orbital relaxation (ΔA)	+0.47	−0.17	+0.14	–	−0.51	+0.20	−0.31	−0.17
Total atomic deformation ($\Delta D = \Delta R + \Delta A$)	**+2.21**	**+3.21**	**+8.62**	–	−12.35	+2.57	**−9.78**	**−1.16**

See footnote of Table 1, in particular the asterisk

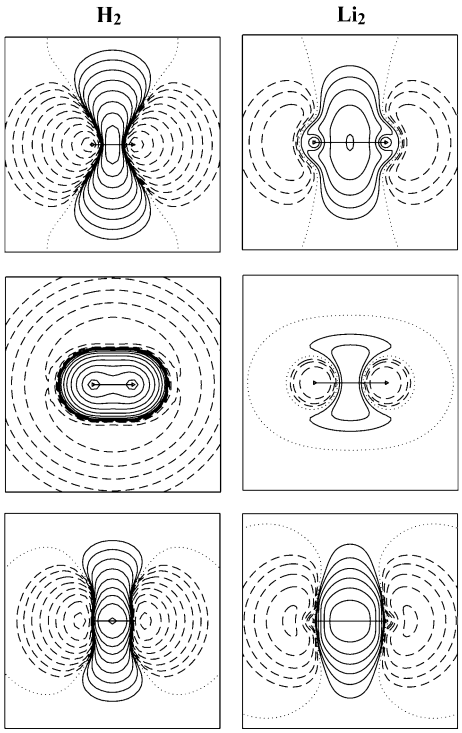

Fig. 3 Density changes upon molecule formation. *Left*: $2H \rightarrow H_2$. *Right*: $2Li \rightarrow Li_2$. Contour line values are $\pm 0.000675 \cdot 2^n$ e/Å^3, $n = 0, 1, 2,\ldots$ *Dashed lines* are negative, zero line is *dotted*. *Top*: Interference of undeformed AOs (frozen LCAO). *Middle*: Atomic radial deformation. *Bottom*: Atomic angular deformation (polarization). (The sum is the total molecular difference density, e.g., in Fig. 2 right).

4.1.1 The overlay level

As in H_2^+, there is slight quasiclassical potential repulsion $V(\Delta C)$, and the bond-parallel interference stabilization by $T_{\parallel}(\Delta I)$ dominates over $T_{\perp}(\Delta I)$. The smaller absolute values for Li have two origins. One is the large extension of the 2*s* AO. The other one is the shape of the effective pseudo-potential. The electron-attracting potential around a proton is deep (Fig. 2 left), giving rise to large kinetic energy contributions. In atoms with occupied core shells, the Pauli principle prevents valence electrons (of same angular momentum as in the core) to accumulate significant density near the attracting nucleus, at the expense of high *kinetic* energy. In the pseudo-potential approach, this kinetic energy increase is simulated by the repulsive pseudo-*potential*, which counteracts the attractive electrostatic part of the core potential. Pseudo-potential calculations yield (approximately) the same observable total energies as ab initio calculations, but in a picture with smaller potential and kinetic energies for the pseudo-valence orbitals.

In Fig. 4, the effective pseudo-potential of the two Li^+ cores in Li_2^+ is shown. Strictly speaking, the pseudo-potential is a nonlocal operator, which cannot be plotted in ordinary space [57, 58]. So, what we plot here is the pseudo-potential that acts on a pure *s* orbital centered on the nearest nucleus. The pseudo-potential for p orbital contributions to the MO is different, especially for second row atoms. However, if we absorb the centrifugal pseudo-potential $l(l+1)/2r^2$ into the kinetic Pauli pseudo-potential, the potentials for *s* and *p* contributions become rather similar. We note that this similarity is the reason of the exceptional tendency toward *s–p* hybridization in the middle of the second row (in particular of the C atom) that had been highlighted before by Kutzelnigg [54–56].

The interference density change raises the potential energy in H_2^+, whereas this does not happen in Li_2^+. Again, the reason is the different pseudo-potential (compare Figs. 2 and 4). In the hydrogen and lithium cases, there occurs electronic charge concentration in the bond center, and this density comes from where it is ordinarily found in the atoms, i.e., from the potential wells. But for lithium that is no longer the nuclear region, but the 'bottom of the spatial 2*s* shell' just outside the core. Consequently, there is nearly no potential energy change upon interference in Li_2^+, see Fig. 4 left.

Table 3 Pseudo-potential energy decomposition (in eV) of Li_2^+ at $R = 5.8$ au $\approx R_e$

Li_2^+	$T_{\parallel}$	$T_{\perp}$	T	V_{cc}	V_{ce}	V	E
Separated atoms	+0.71	+0.71	+2.13	–	−7.52	−7.52	−5.39
Molecule	+1.29	+1.12	+3.52	+4.69	−14.88	−10.19	−6.67
Bond energy ($\Delta E = \Delta O + \Delta D$)	**+0.58**	**+0.41**	**+1.39**	+4.69	−7.36	**−2.68**	**−1.28**
Quasiclassical interaction (ΔC)	–	–	–	+4.69	−4.48	+0.21	+0.21
Quantum interference (ΔI)	−0.34	−0.08	−0.50	–	−0.02	−0.02	−0.51
Total overlay effect ($\Delta O = \Delta C + \Delta I$)	**−0.34**	**−0.08**	**−0.50**	+4.69	−4.49	**+0.20**	**−0.30**
Radial orbital relaxation (ΔR)	+0.14	+0.29	+0.71	–	−0.97	−0.97	−0.25
Angular orbital relaxation (ΔA)	+0.78	+0.20	+1.17	–	−1.90	−1.90	−0.73
Total atomic deformation ($\Delta D = \Delta R + \Delta A$)	**+0.92**	**+0.49**	**+1.88**	–	−2.87	**−2.87**	**−0.98**

See footnote of Table 1

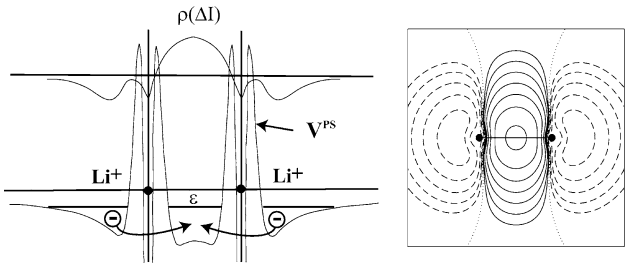

Fig. 4 *Left*, bottom: Pseudo-potential function V^{ps} along the internuclear axis for a valence electron in the field of two lithium cores Li^+ at the equilibrium distance of Li_2^+. Above: Interference density redistribution $\rho(\Delta I)$. The bond charge concentration in the center of Li_2^+ hardly changes the potential energy value. *Right*: Difference density ($Li_2 - 2Li$), contour line values are $\pm 0.000675 \cdot 2^n$ e/Å^3, $n = 0, 1, 2,\ldots$ *Dashed lines* are negative, zero line is *dotted*

4.1.2 Atomic deformation

Remarkably, orbital deformation is similarly efficient in Li_2^+ and H_2^+, about 1 eV in both cases, although the total bond energy of Li_2^+ is less than half that of H_2^+. This means, *atomic deformation becomes a major effect* in Li_2^+ bond formation. However, whereas deformation in H_2^+ is mainly radial contraction, it is predominantly angular deformation in Li_2^+ (compare also H_2 and Li_2 in Fig. 3). One may attribute this to the $2s$–$2p$ near degeneracy in the L shell, it is also evident from the shape of the pseudo-potential in Fig. 4. The contraction toward the point of lowest pseudo-potential in Li_2^+ is *contraction toward the bond center*, while in hydrogen it is contraction toward the nuclei (Fig. 2). The latter is achieved by AO radial scaling, $e^{-r} \rightarrow e^{-\alpha r}$, $\alpha > 1$. In the Li pseudo-potential case, radial scaling does not help, since it would press electron density into the core against the repulsive part of the pseudo-potential. In ab initio calculations, orbital orthogonalization prevents inappropriate core penetration of the valence electrons. If we interpret the H-orbital scaling as $e^{-r} \rightarrow (e^{-r})^{\alpha}$, the concept becomes applicable to pseudo-potential calculations, too, and turns out to be quite effective. Orbital φ^{α} with exponent $\alpha > 1$ is raised, where φ is large (and that is so, where the potential is deep), and is reduced where φ is small. This is just the type of deformation, which the virial theorem demands: raising of kinetic energy and lowering of potential energy, by amplitude concentration in deep potential regions. We achieved this computationally by linear combination of the AO and the squared AO.

4.2 The Li_2 molecule (Table 4)

As for H_2, the quasiclassical interaction is slightly attractive, though this time only because of correlation. Namely, the Li^+ cores exert a Pauli pseudo-repulsion on the overlaid valence shells of the other atom of about +0.3 eV. The dominant sharing effect is the interference lowering of $T_{\|}$, again slightly less than twice that of Li_2^+, similar to the hydrogen case. The potential energy change due to the sharing interference bond charge (Fig. 3) is slightly repulsive, as in H_2, but becomes attractive after correlation correction.

Orbital deformation in Li_2 is much less efficient than in Li_2^+. The reason is electron crowding in the middle of the Li_2 molecule, while in H_2 the density contracts to the two nuclear centers (Fig. 3). Accordingly, electron correlation is different in H_2 and Li_2. In H_2 with two potential wells, the dominant type of correlation is left–right. In Li_2 with a single trough in the molecular center, angular correlation is the dominant one, see Table 5.

Another, at first sight puzzling, difference between lithium and hydrogen had been noticed by Müller and Jungen [77]. In H_2 and H_2^+, $T_{\|}(\Delta E)$ is lower than in the atom H, while $T_{\perp}(\Delta E)$ has strongly increased. But in Li_2^+, $T_{\|}(\Delta E)$ is higher than in the atom and is even higher than $T_{\perp}(\Delta E)$. Again, the reason is the shape of the pseudo-potential. In H_2^+, radial contraction increases both $T\|$ and $T_{\perp}$ similarly. Since sharing interference had decreased $T\|$ so much, it remains quite low in the molecule. In Li_2^+,

Table 4 Pseudo-potential energy decomposition (in eV) of Li_2 at $R = 5.05$ au $\approx R_e$

Li_2	$T_{\|}$	$T_{\perp}$	T	V_{cc}	V_{ce}	V_{ee}	V	E
Separated atoms	+1.42	+1.42	+4.27	–	−15.06	–	−15.06	−10.78
Molecule	+1.44	+1.47	+5.26*	+5.39	−27.16	+6.39	−17.11*	−11.84*
Bond energy ($\Delta E = \Delta O + \Delta D$)	**+0.02**	**+0.05**	**+0.99***	+5.39	−12.10	+6.39	**−2.05***	**−1.06***
Quasiclassical interaction (ΔC)	–	–	–	+5.39	−9.85	+4.65	−0.68*	−0.68*
Quantum interference (ΔI)	−0.56	−0.11	+0.10*	–	−0.34	+1.11	−0.10*	−0.01
Total overlay effect ($\Delta O = \Delta C + \Delta I$)	**−0.56**	**−0.11**	**+0.10***	+5.39	−10.19	+5.76	**−0.78***	**−0.69***
Radial orbital relaxation (ΔR)	+0.14	+0.16	+0.47	–	−0.66	+0.09	−0.57	−0.10
Angular orbital relaxation (ΔA)	+0.44	−0.01	+0.43	–	−1.24	+0.54	−0.70	−0.27
Total atomic deformation ($\Delta D = \Delta R + \Delta A$)	**+0.58**	**+0.16**	**+0.90**	–	−1.90	+0.63	**−1.27**	**−0.37**

See footnote of Table 1

Table 5 σ_g^2 valence shell correlation energy contributions: left–right, in–out, and angular in %

Correlation type (config. mixing)	Left–right ($\sigma_g^2 \rightarrow \sigma_u^2$)	Angular ($\sigma_g^2 \rightarrow \pi^2, \delta^2$)	In–out ($\sigma_g^2 \rightarrow {\sigma_g}^2$)
H_2	46	29	23
Au_2	39	40	19
Cs_2	38	43	19
Na_2	35	45	20
Cu_2	32	48	19
Li_2	25	51	24

however, angular deformation by mixing in $p\sigma$ AOs increases $T_\parallel$ three times more than $T_\perp$ so that $T_\parallel$ becomes larger than in the atom and larger than $T_\perp$, although $T_\parallel$ had been significantly lowered by interference in the ΔI step.

5 Further homopolar sigma bonds

The H atom has a medium nuclear attraction, i.e., electronegativity (EN), and no inner core shells. The Li atom differs in two respects. It has an occupied atomic core, and it has a rather low EN with diffuse valence orbital. Typical main group elements (except from the second row of the periodic table) have bigger cores and larger ENs. A representative example with a simple valence *s*–shell, a big core and a significant EN is Au (its EN is similar to that of iodine). We present bond energy analyses of Au_2^+ and Au_2 in Sects. 5.1 and 5.2. The chemically most important nonmetals have medium large cores and valence-active *s–p* shells. We analyze a respective model in Sect. 5.3.

5.1 The Au_2^+ molecular ion (Table 6)

In order to account for the large relativistic effects in the cores of these heavy atoms, a so-called large-core scalar-relativistic energy-adjusted pseudo-potential was applied [31, 32]. When two Au^+ cores approach each other, the valence electron of Au_2^+ becomes shared and the kinetic energy decreases: at the comparatively large internuclear distance of 1¾ R_e by about –½ eV (Table 6), and much more at shorter distances. At shorter distances, however, the pseudo-potential repulsion of the big core against the penetrating valence electron of the other atom sets in. At R_e, the valence electron becomes confined in the low-potential region that has then developed at the bond center (Fig. 5). This potential well is much more pronounced than in Li_2^+ (Fig. 4) with a similar nuclear distance. The well minimum at the bond center of Au_2^+ is lower than the trough around the core of a single Au atom. Therefore, interference charge accumulation in the bond center *reduces* the potential energy in Au_2^+.

As in Li_2^+ with its single potential well, the dominant contribution to the bond energy comes from contraction of the valence MO toward the bond center and toward the low potential just above the atomic cores. This is describable by combined radial density piling up in the inner region of the valence shell and by angular polarization through *s–p* hybridization. It is the sharing interference lowering of T_e that makes this drastic contraction energetically profitable so that the final $T_\parallel$ and $T_\perp$ are both only slightly higher than in the atom.

5.2 The Au_2 molecule (Table 7)

At larger internuclear separations with small overlap, Au_2 and Au_2^+ behave similar. At equilibrium separation, the kinetic sharing stabilization is counterbalanced by the kinetic correlation correction, by electrostatic bond charge repulsion of the two valence electrons, and by core repulsion. We remember that the two-electron bond energy of Li_2 (−1.06 eV) is even smaller than the one-electron bond energy of Li_2^+ (−1.28 eV). Radial AO relaxation of the overlapping Au-6*s* AOs is a complex reorganization with reduction in T_e and V_{ee} and increase in V_{ce} but with small total energy lowering. An important energy lowering comes through angular deformation by *s–p–d* hybridization, corresponding to the stabilization of the bond by the mechanism maintained in many textbooks: bond charge accumulation in the bond center.

Table 6 Pseudo-potential bond energy decomposition (in eV) of Au_2^+ at $R = 5.0$ au $\approx R_e$

Au_2^+	$T_\parallel$	$T_\perp$	T	V_{cc}	V_{ce}	V	E
Bond energy	**+0.20**	**+0.25**	**+0.70**	**+5.44**	**−8.39**	**−2.95**	**−2.25**
Total overlay effect (ΔO)[a]	−0.39	−0.07	**−0.52**	+3.13	−2.83	**+0.30**	**−0.22**
Radial orbital relaxation (ΔR)	+0.22	+0.42	**+1.05**		−2.89	**−1.70**	**−0.65**
Angular orbital relaxation (ΔA)	+0.37	−0.10	**+0.17**		−2.67	**−1.55**	**−1.38**

See footnote of Table 1. [a] The individual positive and negative energy contributions are for $R = 8.7$ au, where their absolute values are not so huge as at R_e, but where the total overlay E is the same

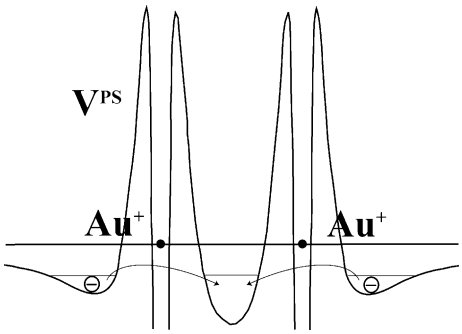

Fig. 5 Pseudo-potential V^{ps} of a valence electron in the field of two Au^+ at the equilibrium distance of Au_2^+ along the internuclear axis. Density concentration at the bond center lowers the potential energy

5.3 A model for *s–s-σ* bonds in a typical E_2 molecule (Table 8)

The chemically more important atoms C and N have spatially smaller cores with larger pseudo-potential values than Li or Au, but their electronegativities are much larger than for Li, even larger than for Au. We create a simple atomic model pseudo-potential for this situation, i.e. for an *s*-type core, which should for simplicity support just a single *s–s-σ* bond: $\hat{V}_E^{ps} = -2/r + \hat{P}_0 \cdot 50\ \exp(-9r^2)$, combined with core-core repulsion $V_{cc} = +1.66/R$. The projection operator $\hat{P}_0$ simulates the orthogonality of valence orbitals onto *s* cores. The shape of the pseudo-potential is as in Li_2 (Fig. 4), but as deep as in Au_2 (Fig. 5) or H_2 (Fig. 2).

At the undeformed AO overlay level, sharing interference reduces *T* (Table 8). The potential well in the middle is deep enough, and the cores are not that big and repulsive, to get a reduction in *V* from interference bond charge concentration. So the common belief, initiated by Slater [74, 75] holds for molecules that are more 'normal' than H_2, namely that the bond charge due to interference of undeformed AOs contributes to electrostatic bond stabilization. But this is not the sole physical origin for stabilizing bond charge accumulation.

A further concentration of charge in the potential well at the bond center occurs by hybridization of the undeformed *s* and *p* AOs, and it further decreases the *V* value. T_e increases only slightly, because $(\nabla\varphi)^2$ is nearly zero anyhow in the overlap region because of contragradience [21]. Further energy improvement, and significant orbital modification toward fulfillment of the virial theorem (with *T* increase and *V* decrease) is achieved by simply mixing in *s* and *p* orbitals with their radial functions squared, as mentioned for Li_2^+. Many permutations of these different energy lowering steps are possible. The respective energy increments in Table 8 are not much dependent on that order (within ±2%); the individual steps still have a reasonably well defined meaning.

Table 8 Energy decomposition for a model of a typical s–s-*σ* two-electron bond, in % of the bond energy

E–E	*T*	*V*	*E*
Bond energy (Δ*E*)	+65	−165	−100
Total overlay effect (Δ*O*)	−23	−34	−58
s–p hybridization	+12	−31	−19
Contraction by mixing in squared AOs	+63	−82	−19
Further orbital relaxation	+12	−17	−5
Total atomic deformation (Δ*D*)	+88	−130	−42

6 Heteropolar sigma bonds

6.1 The one-electron heteropolar bond in LiH^+ (Table 9)

Again, for this molecular ion, there is slight *quasiclassical* repulsion at the undeformed atomic overlay level, but this time there is nearly no sharing energy lowering *E*(CT + Δ*I*). Equal sharing, i.e. *transfer* of half an electron from the more to the less electropositive atom, is too energy expensive. Also from inspection of the effective potential (Fig. 6), one understands that only little charge transfer from H to Li^+ will occur with only little *V* increase. The electronegativity difference impedes *sharing*, which in the present case would hardly increase the available space for the electron. So there is only little *T* decrease. The minimal basis LCAO approximation does not yield bonding, i.e. *E*(LCAO) is slightly positive. In

Table 7 Pseudo-potential bond energy decomposition (in eV) of Au_2 at $R = 4.67$ au $\approx R_e$

Au_2	$T_\parallel$	$T_\perp$	***T***	V_{cc}	V_{ce}	V_{ee}	***V***	***E***
Bond energy	**−0.4**	**+0.2**	**+0.6***	**+5.8**	**−14.2**	**+6.7**	**−3.0***	**−2.3***
Total overlay effect (Δ*O*)[a]	−0.2	−0.0	**+0.3***	+2.2	−8.4	+5.8	**−1.6***	**−1.3***
Radial orbital relaxation (Δ*R*)	−0.5	−0.5	**−1.5**		+1.6	−0.2	**+1.4**	**−0.1**
Angular orbital relaxation (Δ*A*)	+0.4	+0.7	**+1.7**	3.6	−7.5	+1.1	**−2.8**	**−1.0**

See footnote of Table 1. [a] The individual positive and negative energy contributions are for $R = 12.3$ au, where their absolute values are not so huge as at R_e, but where the total overlay *E* is the same

Table 9 Pseudo-potential energy decomposition (in eV) of LiH^+ at $R = 4.06$ a.u. $\approx R_e$

LiH^+	T	V	E
Separated atoms (H, Li^+)	+13.61	−27.21	−13.61
Molecule	+13.58	−27.33	−13.75
Bond energy (ΔE)	**−0.03**	**−0.12**	**−0.14**
Quasiclassical interaction (ΔC)	–	+0.07	+0.07
(CT + ΔI) from LCAO	−0.20	+0.20	0.00
Total LCAO overlay effect (ΔO)	**−0.20**	**+0.27**	**+0.07**
Radial orbital relaxation (ΔR)	+0.39	−0.43	−0.04
Angular orbital relaxation (ΔA)	−0.21	+0.03	−0.17
Total atomic deformation (ΔD)	**+0.18**	**−0.40**	**−0.22**

See footnote of Table 1

Au_2^+, electron repulsion by the big cores cancels the sharing reduction in T; in Li_2, the interelectronic repulsion in the bond center cancels the overlay energy reduction; in LiH^+, there is hardly any sharing. Pauling [78] noted already in 1931 that resonance *of a single* electron between significantly different atoms is impossible (see also Refs. [79–81]). Accordingly, radial contraction is also weak and energetically inefficient. The main effect of bonding is the polarization of the highly populated H-1*s* and the weakly populated Li-2*s* AOs toward the 'bond center'. Consequently, the bond remains of secondary, polarization type.

6.2 The two-electron heteropolar bond in LiH (Table 10)

Due to the repulsive Li^+ core potential, there is weak quasiclassical repulsion of H by overlaid Li. This is turned into slight stabilization (as in Li_2 or model-E_2, though not yet in Au_2), if correlation of the two valence electrons is accounted for ($E(\Delta C)$). With one electron on each atom, a large interference lowering of T occurs ($T(\Delta I)$, Table 10), in magnitude between those of Li_2 and H_2. Since the interference shifts charge from the density maximum at the proton toward the molecular center, $V_{ce}(\Delta I)$ rises (Fig. 6). The accumulation of two electrons in the same region raises V_{ee} even more. If we relax the frozen atomic populations and allow for charge transfer from Li to H within the undeformed minimal valence AO basis set, charge moves from the diffuse Li-2*s* to the compact H-1*s* shell. This implies large T(CT) increase and even larger V(CT) decrease. A large fraction of the bond energy is due to the polarity of this bond, which may be interpreted as partially ionic. However, we note the point of Dunitz [62, 82] that the working of an ionic model does not imply that ionicity is a property inherent to nature.

The density increase on H and density decrease on Li call for AO deformation [83]. $Li^{\delta+}$ orbital contraction and

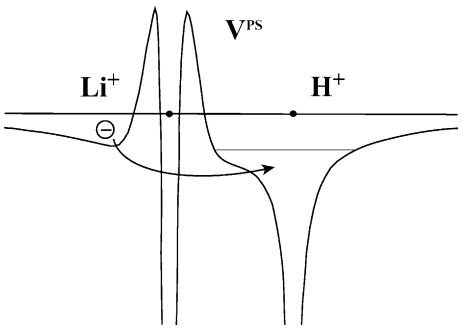

Fig. 6 Effective potential V^{ps} along the internuclear axis for an electron in the field of Li^+ and H^+

$H^{\delta-}$ orbital expansion are to be expected. However, it is already known from Ransil [84] that simple scaling is not very effective, even not for H-1*s*. Radial deformation by a flexible *s*-AO basis is needed for long range contraction without simultaneously increasing the logarithmic derivative of the wave function around the nucleus (that would violate the cusp condition) and without increasing the valence density in the occupied core shell. Complex radial and angular deformations are similarly important and contribute one-third to the total bond energy ($E(\Delta D)$ in Table 10).

The one-electron bond in a homonuclear diatomic A_2^+ is stronger than half the two-electron bond in A_2, because electron–electron repulsion destabilizes the two-one-electron covalences in A_2. Typically $\gamma = BE(A_2^+)/BE(A_2)$ is between 0.6 and 1.3, i.e., the one-electron bond may be even stronger than the two-electron bond (Table 1 of part I) [5]. Lewis was astonished, when he found so many electron pair bonds that he even suspected the breakdown of the Coulomb repulsion law at molecular interelectronic distances [25]. On the other hand, γ is smaller than 0.5 for the polar and the correlative (e.g., 'charge fluctuating' [85–89]) bonds in LiH, NaCl, HF, and F_2. Two-electron bonding in a polar system A:B gets a large contribution from ionic A^-B^+ attraction, and in addition, electron repulsion supports sharing interference for each of the two-one-electron covalences. On the other hand, there is little sharing in polar $A{\cdot}B^+$ systems between the electron-attracting and the electropositive atoms, what illuminates the 'paradoxical role of electron repulsion' to stabilize the polar pair bond. An important point in comparisons of neutral molecules |A:B| with their cations AB^+ is the difference between the loss of a bonding electron in $|A{\cdot}B|^+$ or of a lone-pair (or core) electron in $\cdot A{:}B|^+$ or in $|A{:}B{\cdot}^+$. In the case of polar molecules $[|A^+ :B|^-]$, e.g., the cations $[{\cdot}A^{2+}{:}B|^-]^+$ and $[|A^+{:}B{\cdot}]^+$ will have stronger or weaker bonds, respectively [90, 91]. This aspect is sometimes missed in respective bond discussions [92].

Table 10 Pseudo-potential energy decomposition (in eV) of LiH at $R = 3.01$ a.u. $\approx R_e$

LiH	T	V_{cc}	V_{ce}	V_{ee}	V	E
Separated atoms	+15.74	–	−34.74	–	−34.74	−19.00
Molecule	+18.66*	+9.04	−60.37	+13.11	−40.18*	−21.52*
Bond energy (ΔE)	**+2.92***	+9.04	−25.64	+13.11	**−5.44***	**−2.52***
Quasiclassical interaction (ΔC)	–	+9.04	−15.68	+6.83	−0.78*	−0.78*
Quantum interference (ΔI)	−2.48*	–	+0.73	+2.76	+2.52*	+0.04
Charge transfer (CT)	+5.97	–	−9.95	+3.03	−6.92	−0.95
Total overlay effect (LCAO)	**+3.49***	+9.04	−24.90	+12.62	**−5.18***	**−1.69***
Radial orbital relaxation (ΔR)	−1.30	–	+0.88	+0.06	+0.94	−0.36
Angular orbital relaxation (ΔA)	+0.72	–	−1.61	+0.42	−1.18	−0.47
Total atomic deformation (ΔD)	**−0.57**	–	−0.74	+0.49	**−0.26**	**−0.83**

See footnote of Table 1

6.3 The s–p-σ pair bond in BH (Table 11)

Significant quasiclassical electrostatic attraction occurs when the H-1s penetrates into the inner part of the valence shell of B-$2s^2 2p\sigma^1$, where the $1s^2$ core of B^{3+} is only weakly shielded (Table 11, $V(\Delta C) = -2.15$ eV). The Pauli-repulsive overlap of H-1s with B-$1s^2$ is small and amounts to only +0.25 eV.

At the quantum–mechanical undeformed minimal basis LCAO level ($\Delta I + \Delta P$), several things happen. (i) Keeping H-1s outside the B core raises both T and V a little. (ii) B-2p-H-1s sharing interference leads to the typical lowering of T, especially of the large $T_{\|}$ component. (iii) 0.2 electrons are 'promoted' from B-2s to B-2$p\sigma$. This creates a quadrupolar difference density (Fig. 7, middle) with respect to spherically averaged B-$1s^2 2s^2\ 2p_x^{1/3} p_y^{1/3} 2p_z^{1/3}$ [93–101]. (iv) Polar charge transfer is small (0.04 e) corresponding to the small electronegativity difference of B and H.

The common quadrupolarity of bonded p-block atoms [60–62, 82, 93–101] has an interesting classical analogy. The valence electrons are floating on the atomic core, like ocean water on the earth. A second attractive center (the other atom, or the moon, respectively) causes two low and two different high tides (Fig. 7, right). The s–p promotive density deformation increases T. In the pseudo-potential approach, B-2s has a smaller kinetic energy than B-2p, since the pseudo-2s AO has no radial node, and of course also no angular node. V_{ee} is reduced, because s–p hybridization shifts the B-$2s^2$ lone-pair away from the B–H bond pair.

Orbital deformation behaves as expected, with T_e and V_{ee} increase and V_{ce} decrease, due to radial contraction toward the proton and toward the potential valley 'just above' the B core and due to polarization toward the bond center. The effective potential in BH (Fig. 7, left) is similar to the one in LiH (Fig. 6), but much deeper around the B^{3+} core and at the bond center. Therefore, and in contrast to LiH, the HOMO energy level allows for valence density at the backside of the boron as shown in Fig. 7, middle.

7 Bonds involving pσ and pπ orbitals

7.1 The p–p-σ bond in B_2 (Table 12)

The ground state $(\sigma_g^2\sigma_u^2\pi_{ux}\pi_{uy})\ ^3\Sigma_g^-$ of B_2 contains two-one-electron pπ–pπ bonds. We here analyze the excited $(2s\sigma_g^2 2s\sigma_u^2 2p\sigma_g^2)^1\Sigma_g^+$ state with a single ppσ pair-bond. The quasiclassical overlay attraction $V(\Delta C) = -2¾$ eV is nearly twice the total bond energy $E(\Delta E) = -1½$ eV (Table 12). At the ab initio level, the classical electrostatic overlay attraction would be even bigger (nearly −5 eV) but is compensated by an additional quantum kinetic energy increase, corresponding to the orthogonalization of the atomic valence orbitals on the other atom's occupied shell. As in BH, valence density from the other atom penetrates the filled $2s^2$ shell and becomes attracted by the B^{3+} core.

The dominant effect described at the undeformed LCAO approximation is the energy increase due to Pauli repulsion, i.e., orthogonalization on 2s. It means a depopulation of 2s and a promotion to 2p of 0.17 e per atom. Thereby T, especially $T_{\|}$, is increased, as in the case of BH. Even after inclusion of correlation and sharing interference, the interaction energy is still slightly positive (E(LCAO) = +0.4 eV). Only after accounting for atomic deformation, one gets some bonding. It is not very strong, corresponding to the fact that $(2p\sigma_g^2)^1\Sigma_g^+$ is an excited state with the same dissociation limit as the $(2p\pi^2)^3\Sigma_g^-$ with a more common bond energy of −3.1 eV. Still, $2p_\sigma$ electron sharing is one important factor in B_2 σ-bonding, while 2s Pauli repulsion partially compensates the T lowering. Because of computational simplicity, the promotional energy terms (ΔP in Table 12) were determined *before* interference.

Table 11 Pseudo-potential energy decomposition (in eV) of BH at $R = 2.43$ au $\approx R_e$

BH	$T_{\parallel}$	$T_{\perp}$	$\boldsymbol{T}$	$V_{cc} + V_{ce}$	V_{ee}	$\boldsymbol{V}$	$\boldsymbol{E}$
Separated atoms	+22.85	+14.47	+51.80	−169.87	+34.61	−135.25	−83.46
Molecule	+23.04	+16.20	+56.25*	−219.14	+66.26	−143.27*	−87.03*
Bond energy (ΔE)	**+0.19**	**+1.73**	**+4.45***	−38.07	+31.65	**−8.02***	**−3.57***
Quasiclassical interaction (ΔC)	–	–	–	−31.50	+30.15	−2.15*	−2.15*
Interference (ΔI) + promotion (ΔP)	−1.97	−0.46	−2.08*	+4.42	−1.53	+2.09*	+0.01
Total LCAO overlay effect	**−1.97**	**−0.46**	**−2.08***	−27.08	+28.62	**−0.06***	**−2.14***
Radial orbital relaxation (ΔR)	+1.06	+1.70	+4.45	−7.72	+2.28	−5.44	−0.99
Angular orbital relaxation (ΔA)	+1.10	+0.49	+2.08	−3.27	+0.75	−2.51	−0.44
Total atomic deformation (ΔD)	**+2.16**	**+2.19**	**+6.53**	−10.99	+3.03	**−7.95**	**−1.43**

See footnote of Table 1

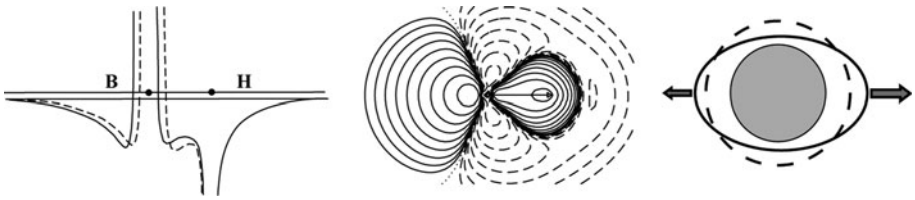

Fig. 7 *Left*: Effective potential along the internuclear axis of BH for a valence electron: *solid line* V^{ps} of an electron in *s*-AOs; *dotted line* $V^{ps} + 1/r^2$ (centrifugal potential) of an electron in B *p*-AOs. *Middle*: Difference density between BH molecule and spherical B, H atoms. Contour line values $\pm 0.000675 \cdot 2^n$ e/Å^3, $n = 1, 2, \ldots$. Dashed lines are negative. *Right*: The tide effect: The moon assumed on the right attracts the ocean, on the right more and on the left less than in the middle, where the attraction force is as for the whole earth

Table 12 Pseudo-potential energy decomposition (in eV) of B_2 ($\sigma_g^2\ ^1\Sigma_g^+$) at $R = 3.51$ au $\approx R_e$

B_2 ($^1\Sigma_g^+$)	$T_{\parallel}$	$T_{\perp}$	$\boldsymbol{T}$	$V_{cc} + V_{ce}$	V_{ee}	$\boldsymbol{V}$	$\boldsymbol{E}$
Bond energy (ΔE)	**+3.38**	**+1.88**	**+7.94***	−73.57	+65.70	**−9.47***	**−1.53***
Quasiclassical interaction (ΔC)	–	–	–	−71.53	+69.57	−2.76*	−2.76*
Promotion (ΔP)	+3.32	+0.47	+4.26	+9.13	−9.74	−0.62	+3.64
Interference (ΔI)	−0.41	−0.04	+0.30*	−3.47	+3.49	−0.78*	−0.47
Total LCAO overlay effect	**+2.91**	**+0.43**	**+4.57***	−73.62	+63.32	**−4.16***	**+0.41***
Radial orbital relaxation (ΔR)	−2.16	−0.04	−2.25	+2.23	−0.91	+1.32	−0.93
Angular orbital relaxation (ΔA)	+2.63	+1.49	+5.62	−9.93	+3.29	−6.63	−1.01
Total atomic deformation (ΔD)	**+0.47**	**+1.45**	**+3.37**	−7.70	+2.38	**−5.31**	**−1.94**

See footnote of Table 1

Atomic radial and angular deformations are both important for bonding. The unfavorable $T_{\parallel}$ contribution (mainly from $2s\sigma_u$) is significantly reduced by a flexible *s*-AO basis, this time corresponding to radial *expansion*. Two-thirds of the angular deformation is obtained with a more flexible p-AO basis, allowing *contraction* toward the bond center and toward the boron nuclei (there is no repulsive pseudo-potential acting on *p*-AOs of the same center). We note the similarity between *s*-contraction in *s*–*s*-σ bonded H_2 and *p*-contraction in *p*–*p*-σ bonded B_2.

The total bond energy comes from the *interplay* of electrostatic attraction, Pauli repulsion, sharing interference attraction, and energy lowering due to atomic relaxation. It makes no sense to ask the question, whether it is this or that single term that causes bonding. Bonding will occur, if at least some attractions are 'comparatively' strong and have a pronounced tendency to lower the total energy, and the repulsions are 'comparatively' weak and do not prevent bonding, in a variational regime.

7.2 The p–p-σ and p–p-π bonds in N_2 (Table 13)

In addition to one 2e-σ bond ($\sigma_g^2\sigma_u^2\sigma_g^2$), N_2 has two 2e-π bonds (π_u^4). The large positive repulsion between the N^{5+} cores is partitioned according to the number of σ and π electrons and combined with the large decreases in $V_{ce,\sigma}$ and $V_{ce,\pi}$ (see Fig. 8). As in B_2, the quasiclassical attraction forms a large fraction of the bond energy (Table 13). In an

Table 13 Pseudo-potential energy decomposition (in eV) of N_2 at $R = 2.068$ au $\approx R_e$

N_2	T_σ	T_π	T	$0.4V_{cc} + V_{ce,\sigma}$	$0.6V_{cc} + V_{ce,\pi}$	V_{ee}	V	E
Bond energy (ΔE)			**+13.72***	$\sigma + \pi = -320.16$		+305.95	**−23.61***	**−9.89***
Quasiclassical (ΔC)	−	−	0	−196.50	−102.49	+296.53	−7.17*	−7.17*
Promotion (ΔP)			+17.13	$\sigma + \pi = +25.40$		−30.86	−5.46	+11.66
Interference (ΔI)	+1.68	−38.71	−32.33*	−14.98	+31.37	+13.59	+25.27*	−7.05
Total overlay effect (ΔO)			**−15.20***	$\sigma + \pi = -257.20$		+279.26	**+12.65***	**−2.56***
s-AO relaxation	$T_\parallel$: − 3.83	$T_\perp$:1.47	−0.89	$\sigma + \pi = -4.78$		+2.81	−1.98	−2.86
p-AO relaxation	+18.12	+10.61	+28.73	−29.20	−19.61	+17.77	−31.03	−2.31
d- and *f*-contributions	+1.02	+0.05	+1.08	−2.48	−6.88	+6.12	−3.23	−2.15
Total atomic deformation (ΔD)	**+18.25**	**+10.66**	**+28.92**	$\sigma + \pi = -62.95$		+26.70	**−36.24**	**−7.32**

See footnote of Table 1

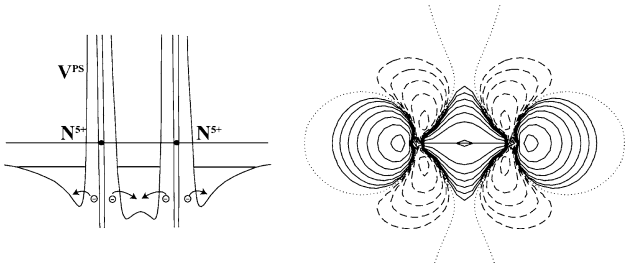

Fig. 8 N_2 *Left*: Effective potential V^{ps} along the internuclear axis for a valence electron in the field of two N^{5+} cores at the molecular distance. Bond charge concentration lowers the potential energy. *Right*: Molecular difference density. Contour lines $\pm 0.025 \cdot 2^n$ e/A^3, $n = 0, 1, 2, \ldots$ *Dotted line*: zero, *dashed lines*: negative

ab initio approach without $1s^2$ Pauli repulsion, there is an additional large electrostatic attraction. The important electrostatic attractions of overlaid atoms in covalences have been highlighted recently [40, 76].

At larger distances, both σ and π interferences reduce T. However, at the frozen LCAO level, the additional π bonds in N_2 compress the molecule so much that at equilibrium separation, the σ-system raises the T even more than in B_2. The significant interference lowering of T comes from π. The corresponding charge transfer from the atomic pπ region to the midplane of the molecule (Fig. 9) is the π-analogue of the σ-interference density in H_2 (Fig. 3). There is also potential energy increase due to bond charge build up in both cases. The slight bond energy at the frozen LCAO level is due to electron correlation.

Again, atomic deformation in the molecule contributes a lot to bonding. Flexibilization of the *s*-AO basis, of the *p*-AO basis, and additional higher-*l* polarization functions each contribute about one-third. At the end, the molecular T_e is above the atomic values, in accordance with the virial theorem. However, the σ and π systems contribute differently to achieve that aim. The σ system is responsible for a large part of potential energy lowering by contraction toward the bond axis and the surface of the N-$1s^2$ cores, with significant increase in T_σ. The π system contributes mainly to the reduction in kinetic energy density by sharing, and the deformation is dominantly *d*–*f*-polarization. Our simple model of Sect. 3.3 does no longer work well for such a strongly coupled system of two different bond types.

8 A tentative synthesis

One of the fascinating aspects of Chemistry is that there seems to be an endless diversity of different bonding situations, and it is therefore not surprising that our brief sampling of diatomic molecules has also revealed a variety of different bonding patterns.

One among the various approaches to classify bonds on a theoretical basis is to analyze *actual* electronic wavefunctions or their density distributions (in the latter case, experimental densities can also be used [102]). While such taxonomies are useful in a number of contexts, they inherently cannot address the question of *how and why* the underlying physical forces, governed by the relevant physical equations, interact to generate the various bonding situations. The ability of such an approach to elucidate differences is therefore limited. It is just the explanation of distinctions that has been the focus of the present analysis.

One important question is What are the roles played in the formation of bonds by the kinetic and by the nuclear-electron and electron–electron potential energies? Because the variation principle entails the stationarity of the *total* energy of the exact wavefunctions of atoms and molecules, even relatively simple theoretical approximations can typically provide semi-quantitative accuracy for the total bond energy and therefore yield some insight into physical mechanisms. They do not yield, however, reliable information regarding the kinetic and potential energy changes

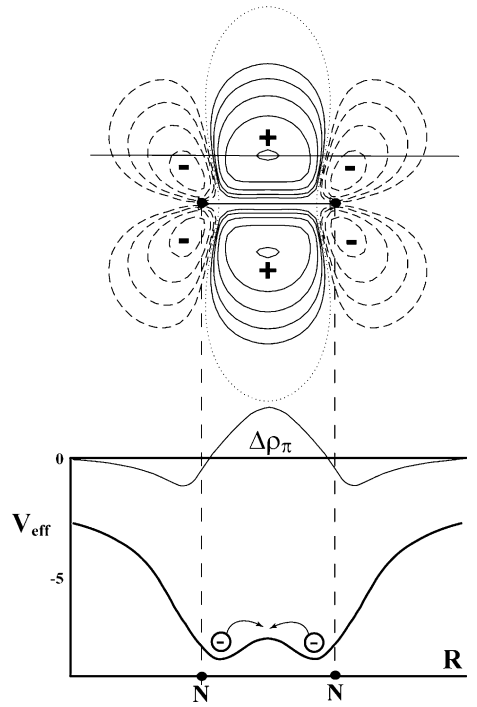

Fig. 9 π-electrons in N_2. *Top*: density difference between a doubly occupied $\pi_{u,x}$-MO of N_2 and two singly occupied p_x-AOs of two *N* atoms at their molecular positions. Contour line values are $\pm 0.025 \cdot 2^n$ e/Å^3, $n = 0, 1, 2, \ldots$ *Dashed lines*: negative. *Bottom*: effective potential of an electron in the field of two *N*-cores along the line indicated above, parallel to the bond axis at a distance of 0.4 Å and π-density change $\triangle\rho_\pi$ along that line

nor regarding such terms as the Hellmann and Ehrenfest forces [103–107]. A more thorough analysis, rigorously based on the variation principle, has therefore been the aim of the present inquiry.

To perform such an analysis for a bond between atoms A and B, one has to relate the wavefunction of the systems (A&B) and (A–B) in some way. This can be effectively achieved by considering physically appropriate *intermediate* wavefunctions along a "variational path in function space." We have found it useful to choose the "overlaid undeformed atoms" as the main intermediate wavefunction and thus distinguish two major steps from (A&B) to (A–B): the *overlay step* and the *relaxation step*. The former contained a *quasiclassical* and an *interference contribution*. The latter contained a *radial* and an *angular* deformation.

The interplay of the various factors for bond formation in the systems examined, which is summarized in Table 14, shows the following. Covalent bonds can be dominated either by the *interaction of the undeformed overlaid atoms* or by the *relaxation of the overlaid atoms in the molecule*. In the former case, the leading term may be the quantum–mechanical *reduction in the kinetic energy pressure due to electron sharing* or the *electrostatic attraction due to overlapping, correlated electronic shells* ('potential-triggered covalence'). Even in the latter case, however, the reduction in the kinetic energy density by electron sharing constitutes an important ingredient, in that it makes a short internuclear distance feasible (e.g., in N_2). The *angular deformation of the overlaid atoms* plays a comparatively small role in H_2, but is usually more important, in particular in short multiple bonds (e.g., in N_2). In some cases, *radial deformation* (often more involved than simple contractive scaling) is more important; in other cases, *angular polarization* is more important. There is also competition of *s- versus p*-overlap and of radial *versus* angular changes.

A major reason for these differences is that the regions of low pseudo-potential differ from molecule to molecule. In the case of hydrogen, they are located near the nuclei. In the case of more loosely bound valence electrons, as in Li-σ and N-π, they lie at some distance from the nucleus around the core shells. In the case of Au-σ and N-σ, they lie at the bond center. In the case of two atoms with different electronegativities and/or core sizes, the molecular pseudo-potential exhibits a strong bias toward one nucleus, as in LiH and BH.

An additional factor of influence is the *Pauli repulsion between closed shells*, be they *core or lone-pair* shells. Upon A–B bond formation, the singly and doubly occupied valence orbitals of A overlap with the singly and doubly occupied valence orbitals and with the doubly occupied core orbitals of B, and vice versa. While the pseudo-potential approach has eliminated the core effects on the same atom, there still remain the repulsions between the valence orbitals on A and the Pauli-forbidden regions of B. These orbital orthogonality effects lead to significant orbital modifications and yield significant repulsive contributions to the kinetic and potential energies.

In simple cases, the factors mentioned can be modeled by the parameterized expression (18) of Sect. 3.3, *viz.*

$$E_{\mathrm{mol}}(k, \kappa, Z, \pi, v) = (1 - \kappa) \times k/(2\,\alpha^2) - (1 + \pi/2) \times Z/(v\,\alpha^v). \qquad (24)$$

Figure 10 represents an attempt to place the various discussed bonds in the κ-π-parameter space. The figure also has a further dimension Δ that indicates deviations from the model. For cases were the deviations are too large, different schemes of bond indicators may be useful that highlight different characteristics in parallel, even though perhaps masking other aspects. For instance, the valence bond approach emphasizes left–right correlation via strong 'covalent–charge shift' resonance, while undervaluing (though not completely suppressing) electron sharing. Thereby, it can extract certain chemically relevant

Table 14 Valence energy decomposition (in %) of ten different diatomic covalent molecules

Molecule (bond)	Bond energy BE_o ($-\Delta E$) in eV)	% BE_o		Important contributions				
		Molecular overlay of atoms (ΔO)	Deformation of atoms in molecules (ΔD)	Correlated classical Density overlay (ΔC in ΔO)	Overlapping orbital interference (ΔI in ΔO)	$\Delta T_{\|\|}$ contribution (in ΔI)	Radial deformation (ΔR in ΔD)	Angular polarization (ΔA in ΔD)
H_2	4.75	**76**	24	25	**51**	**70**	21	
LiH	2.52	**67**	33	31	36	**98**	14	19
Li_2	1.06	**65**	35	**64**		**53**		25
BH	3.57	**60**	**40**	**60**		**55**	28	
E_2		**58**	**42**			23		
Au_2	2.3	**55**	**45**	**70**				40
H_2^+	2.78	**53**	**47**		**80**	**74**	36	
N_2	9.89	26	**74**	**72**		**Large T_π**	52	22
Au_2^+	2.25	10	**90**				29	61
$B_2(^1\Sigma_g^+)$	1.53	–27	**127**				61	66

Absolute values; without vibrational energy correction. Dominant contributions are in bold face

differences out of specific bonds and reactions that are not as obvious in the MO-CI approach [85–89, 114].[9]

We may view the first physical step of covalent bond formation as a Lewis-type sharing interference, which tends to accumulate charge in the overlap region, along the bond axis for σ-bonds, and "above and below" the bond axis for π-bonds. This typically lowers the *kinetic* energy. In some cases, it can also lower the *potential* energy with respect to the spherically averaged atoms. The accumulated charge comes from regions of high charge density with low pseudo-potential energy. In atoms with small (e.g., N) or absent cores (H) and with valence AOs of small angular momenta (*s*-AOs), it comes from the vicinity of the nuclei, which is energetically expensive. For atoms with larger cores and with valence AOs of higher angular momenta, it comes from the 'backsides' of the atoms, i.e., from regions just outside the core, farther away from the nuclei and away from the "other" atom; this is energetically less expensive. Accordingly, at the level of overlaid undeformed atomic wavefunctions, the *potential* energy changes may vary from slightly antibonding (H_2^+) to strongly bonding (LiH, B_2), depending on the spatial extension of the overlapping AOs and on the detailed shape of the pseudo-potentials. Correspondingly, the parameter π in Eq. (24) can vary from slightly negative to significantly positive. While the contragradient overlap of partially filled valence AOs always lowers the bond-parallel kinetic energy pressure (positive κ-parameter), rearrangements of *s–p* AO populations (hybridization) may reduce or, occasionally, increase the kinetic energy pressure.

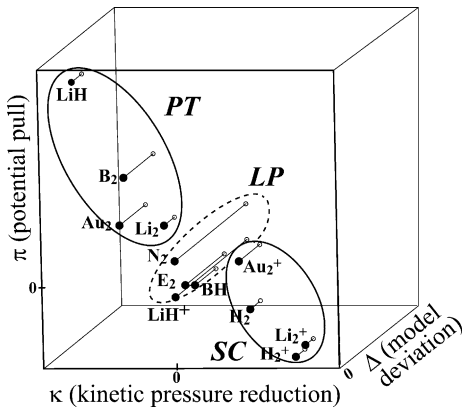

Fig. 10 Different kinds of valences in diatomics (AB means the E_2 of the text) due to three mechanisms, described by three parameters: $\boldsymbol{\kappa}$ = reduced 'kinetic energy pressure' caused by electron delocalization (sharing); $\boldsymbol{\pi}$ = increased 'potential energy pull' caused by charge transfer to more electronegative regions; $\boldsymbol{\gamma}$ = reduced interelectronic repulsion density caused by correlation. $\boldsymbol{\Delta}$ = energy deviation from simple model (Eq. 16). *SC* simple covalences (large $\boldsymbol{\kappa}$; small, even negative $\boldsymbol{\pi}$). *PT* valences with regions of deep potential triggered energy lowering by charge shift (large $\boldsymbol{\pi}$; small, even negative $\boldsymbol{\kappa}$); *LP* covalences interacting with Large Cores or Lone-Pairs (large $\boldsymbol{\Delta}$; small $\boldsymbol{\pi}$ and $\boldsymbol{\kappa}$)

As regards the deformations of the overlaid atoms in the relaxation step, one finds the following possibilities. For hydrogen, without a core, monopolar radial contraction toward the nucleus dominates. In atoms with cores and a single *s*-type valence electron (Li, Au), dipolar density deformation directed toward the bond center dominates. In atoms with cores and several valence electrons in an *s–p* valence shell, the charge flows around the Pauli-repulsive

[9] Interest in the quantum mechanical explanation of the various details of the genesis of various chemical bonds, in addition to their mere description, seems rising in recent years. The importance of local kinetic energy parameters and other wavefunction-based descriptors, the use of different physical definitions of chemical concepts and even the use of chemical "noumena" without uniquely definable physical basis have been advanced [45, 85–89, 115–123]

core and forms a quadrupole with bond and lone-pair densities.

The discussed results exhibit the invalidity of the conjecture that the lowering of the potential energy, which always occurs upon bond formation, is universally caused by the accumulation of electron density between the atoms through orbital overlap. Only in certain special cases, so to speak accidentally, is the assertion valid that "bonding is a result of the lowering of the potential energy in the bonding region caused by the accumulation of density that attracts the nuclei" [108]. In this context, it is interesting to note the fact that the density polarizations near the nuclei, which are caused by the tails of the valence orbitals, dominate in balancing the repulsions between the nuclei [53, 109].

Acknowledgments The authors dedicate this publication to the memory of Professor Jürgen Hinze in appreciation of his personal generosity as well as his scientific contributions, notably to the rigorous foundation of chemical concepts in quantum theory. Thanks are due to S.T. Elbert, P. Valtazanos, and W. Butscher for calculating some numerical values and to M.W. Schmidt for preparing Fig. 1. T.B., K.R. and W.H.E.S. are grateful for the support by Prof. Peyerimhoff during their stay at the University of Bonn in the 1970s, when this work first started. We thank for the support at various times from the Ames Laboratory USDOE at Iowa State University, the University of Bonn, the University of Siegen, and the Shanghai Jiao Tong University. Special thanks go from W.H.E.S. to the late Veronika Ruedenberg for her hospitality in Iowa and Northern Minnesota. This work was financially supported by NATO, USDOE (Division of Chemical Sciences, Office of Basic Energy Sciences, Contract W-7405-Eng-82 with Iowa State University), Fonds der Chemischen Industrie, DAAD, DFG and the Chinese Science Foundation.

References

1. Dunitz JD, Gavezzotti A (2005) Angew Chem 117:1796
2. Dunitz JD, Gavezzotti A (2005) Angew Chem Int Ed 44:1766
3. McNaught AD, Wilkinson A (1997) IUPAC compendium of chemical terminology (Gold Book), IUPAC, Research Triangle Park, NC
4. Nic M, Jirat J, Kosata B (2005 seq.) http://gold.book.iupac.org
5. Bitter T, Ruedenberg K, Schwarz WHE (2007) J Comput Chem 28:411
6. Hellmann H (1933) Z Phys 85:180
7. Hellmann H, Jost W (1934) Z Elektrochem Angew Phys Chem 40:806
8. Hellmann H, Jost W (1935) Z Elektrochem Angew Phys Chem 41:667
9. Hellmann H (1934/1935) Acta Physicochim URSS 1:333
10. Hellmann H (1937) Einführung in die Quantenchemie. Deuticke, Leipzig-Wien. (1944) reprinted. Edwards, Ann Arbor
11. Peierls RE (1955) Quantum Theory of Solids (5.1). Clarendon, Oxford
12. Döring W (1958) Private communication. (1979) Atomphysik und Quantenmechanik, vol III (VI). Walter de Gruyter, Berlin
13. Ruedenberg K (1962) Rev Mod Phys 34:326
14. Feinberg MJ, Ruedenberg K, Mehler E (1970) Adv Quantum Chem 5:27
15. Ruedenberg K (1975) In: Chalvet O, Daudel R, Diner S, Malrieu JP (eds) Localization and delocalization in quantum chemistry, vol 1. Reidel, Dordrecht, p 223
16. Schmidt MW, Ruedenberg K (2007) J Comput Chem 28:391, 2389
17. Kutzelnigg W (1973) Angew Chem 85:551
18. Kutzelnigg W (1973) Angew Chem Int Ed 12:546
19. Kutzelnigg W (1978,1994). Einführung in die Theoretische Chemie. Vol. 2: Die chemische Bindung. VCH, Weinheim
20. Kutzelnigg W (1990) In: Maksíc ZB (ed) Theoretical models of chemical bonding, part 2. The concept of the chemical bond. Springer, Berlin, p 1
21. Goddard WA, Wilson CW (1972) Theor Chim Acta 26:195, 211
22. Fukui K (1976) Kagaku Hannoh to Denshi no Kidoh (Chemical Reactions and Electronic Orbitals). Muruzen, Tokyo
23. Mulliken RS, Ermler WC (1977) Diatomic molecules, Section II. F. Academic Press, New York
24. Ruedenberg K, Schmidt MW (2009) J Phys Chem A 113:1954
25. Lewis GN (1916) J Am Chem Soc 38:762
26. Kossel W (1916) Ann Physik 49:229
27. Bytautas L, Nagata T, Gordon MS, Ruedenberg K (2007) J Chem Phys 127:164317
28. Bytautas, Matsunaga N, Nagata T, Gordon MS, Ruedenberg K (2007) J Chem Phys 127:204301,204313
29. Bytautas L, Ruedenberg K (2009) J Chem Phys 130:204101
30. Merritt JM, Bondybey VE, Heaven MC (2009) Science 324:1548
31. Bitter T (1982) Doctoral Thesis: Zur Deutung und Erklärung der chemischen Bindung in zweiatomigen Molekülen, University of Siegen
32. Bitter T, Schwarz WHE (1976) Ber Bunsenges Phys Chem 80:1231
33. Wang SG, Schwarz WHE (2009) Angew Chem 121:3456
34. Wang SG, Schwarz WHE (2009) Angew Chem Int Ed 48:3404
35. Morokuma K (1971) J Chem Phys 55:1236
36. Kitaura K, Morokuma K (1976) Int J Quantum Chem 10:325
37. Ziegler T, Rauk A (1977) Theor Chim Acta 46:1
38. Ziegler T, Rauk A (1979) Inorg Chem 18:1558, 1755
39. Bickelhaupt FM, Baerends EJ (2000) Rev Comput Chem 15:1, and the references given therein
40. Kovács A, Esterhuysen C, Frenking G (2005) Chem Eur J 11:1813
41. Schwarz WHE (2006) Angew Chem 118:1538
42. Schwarz WHE (2006) Angew Chem Int Ed 45:1508
43. Boča R, Linert W (2005) Monatsh Chem 136:881
44. Gatti C (2005) Z Kristallogr 220:399
45. Ponec R, Gatti C (2009) Inorg Chem 48:11024
46. Kirzhnits DA (1957) Sov Phys JETP 5:64
47. Huang C, Carter EA (2010) Phys Rev B 81:045206
48. Deb BM ed. (1981) The Force Concept in Chemistry. Van Nostrand Reinhold, New York
49. Bader RFW (1990) Atoms in molecules. Oxford University Press, Oxford
50. Francisco E, Martín-Pendás A, Blanco MA (2006) J Chem Theory Comput 2:90
51. Popelier PLA (2005) Struct Bonding 115:1
52. Schwarz WHE, van Wezenbeek EM, Baerends EJ, Snijders JG (1989) J Phys B 22:1515
53. Autschbach J, Schwarz WHE (2000) J Phys Chem. A 104:6039
54. Kutzelnigg W (1984) Angew Chem 96:262
55. Kutzelnigg W (1984) Angew Chem Int Ed 23:272
56. Pyykkö P (2001) Int J Quantum Chem 85:18
57. Schwarz WHE (1968) Theoret Chim Acta 11:307
58. Schwarz WHE (1969) Theoret Chim Acta 15:235
59. Schwarz WHE (1971) Theoret Chim Acta 23:147
60. Bader RFW, Keaveny I, Runtz G (1969) Can J Chem 47:2308
61. Bader RFW, Bedall PM (1972) J Chem Phys 56:3320
62. Dunitz JD, Schweizer WB, Seiler P (1983) Helv Chim Acta 66:123, 134

63. Langmuir I (1919) Proc Natl Acad Sci USA 5:252
64. Heitler W, London F (1927) Z Phys 44:455
65. Sugiura Y (1927) Z Phys 45:484
66. Burrau Ø (1927) Kgl Danske Videnskab Selskab Mat Fys Medd 7(14)1
67. Finkelstein BN, Horowitz GE (1928) Z Phys 48:118,448
68. Hund F (1928) Z Phys 51:759
69. Mulliken RS (1928) Phys Rev 32:186,761
70. Pauling L (1928) Chem Rev 5:173
71. Guillemin V, Zener C (1929) Proc Natl Acad Sci USA 15:314
72. Hylleraas EA (1931) Z Phys 71:739
73. James HM, Coolidge AS (1933) J Chem Phys 1:825
74. Slater JC (1933) J Chem Phys 1:687
75. Slater JC (1963) Quantum Theory of Molecules and Solids. Vol.1 Electronic Structure of Molecules, McGraw-Hill, New York
76. Krapp A, Bickelhaupt FM, Frenking G (2006) Chem Eur J 12:9196, and the references therein
77. Müller W, Jungen M (1976) Chem Phys Lett 40:199
78. Pauling L (1931) J Am Chem Soc 53:3225
79. Feinberg M, Ruedenberg K (1971) J Chem Phys 54:1495
80. Feinberg M, Ruedenberg K (1971) J Chem Phys 55:5804
81. Baird NC, Taylor KF (1980) J Chem Phys 72:6529
82. Dunitz JD, Seiler P (1983) J Am Chem Soc 105:7056
83. Sanderson RT (1983) Polar covalence. Academic Press, New York
84. Ransil BJ (1960) Rev Mod Phys 32:245
85. Shaik S, Danovich D, Wu W, Hiberty PC (2009) Nature Chem 1:443
86. Hiberty PC, Ramozzi R, Song LC, Wu W, Shaik S (2007) Faraday Disc 135:261
87. Hiberty PC, Megret C, Song LC, Wu W, Shaik S (2006) J Am Chem Soc 128:2836
88. Shaik S, Danovich D, Silvi B, Lauvergnat DL, Hiberty PC (2005) Chem Eur J 11:6358
89. Zhang LX, Ying FM, Wu W, Hiberty PC, Shaik S (2009) Chem Eur J 15:2979
90. Schwarz WHE (1974) Angew Chem 86:505
91. Schwarz WHE (1974) Angew Chem Int Ed 13:454
92. Mucci JF, March NH (1981) J Chem Phys 75:5789
93. Schwarz WHE, Ruedenberg K, Mensching L, Miller LL, Jacobson R, Valtazanos P, von Niessen W (1989) Angew Chem 101:605
94. Schwarz WHE, Ruedenberg K, Mensching L, Miller LL, Jacobson R, Valtazanos P, von Niessen W (1989) Angew Chem Int Ed 28:597
95. Schwarz WHE, Mons HE (1989) Chem Phys Lett 156:275
96. Schwarz WHE, Ruedenberg K, Mensching L (1989) J Am Chem Soc 111:6926
97. Mensching L, von Niessen W, Valtazanos P, Ruedenberg K, Schwarz WHE (1989) J Am Chem Soc 111:6933
98. Schwarz WHE, Lin HL, Irle S, Niu JE (1992) J Mol Struct THEOCHEM 225:435
99. Irle S, Lin HL, Niu JE, Schwarz WHE (1992) Ber Bunsenges Phys Chem 96:1545
100. Niu JE, Schwarz WHE (1993) J East China Normal Univ Nat Sci 2:48
101. Miller LL, Jacobson RA, Ruedenberg K, Niu J, Schwarz WHE (2001) Helv Chim Acta 84:1907
102. Coppens P (1997) X-Ray charge densities and chemical bonding. Oxford University Press, Oxford
103. Bader RFW (2008) J Phys Chem A 112:13717
104. Bader RFW (2009) J Phys Chem A 113:10391
105. Bader RFW (2006) Chem Eur J 12:2896
106. Hernández-Trujillo J, Cortés-Guzmán F, Fang DC, Bader RFW (2007) Faraday Disc 135:79
107. Bader RFW, Fang DC (2005) J Chem Theory Comput 1:403
108. Bader RFW, Hernández-Trujillo J, Cortés-Guzmán F (2007) J Comput Chem 28:4
109. Spackman MA, Maslen EN (1985) Acta Cryst A 41:347
110. Wang SG, Qiu YX, Schwarz WHE (2009) Chem Eur J 15:6032
111. Wang SG, Qiu YX, Schwarz WHE (2010) Chem Eur J 16 (in press)
112. Russel CA (1971) The History of Valency. Leicester University Press, Leicester
113. Kutzelnigg W, Schwarz WHE (1982) Phys Rev A 26:2361
114. Shaik S, Chen ZH, Wu W, Stanger A, Danovich D, Hiberty PC (2009) Chem Phys Chem 10:2658
115. Anderson JSM, Ayers PW, Rodriguez-Hernandez JI (2010) J Phys Chem A 114 (in press)
116. Ayers PW, Jenkins S (2009) J Chem Phys 130:154104
117. Wu Q, Ayers PW, Zhang YK (2009) J Chem Phys 131:164112
118. Francisco E, Martín-Pendás A, Blanco MA (2009) J Chem Phys 131:124125
119. Khaliullin RZ, Cobar EA, Lochan RC, Bell AT, Head-Gordon M (2007) J Phys Chem A 111:8753
120. Liu SB (2007) J Chem Phys 126:244103
121. Parr RG, Ayers PW, Nalewajski RF (2005) J Phys Chem A 109:3957
122. Tachibana A (2001) J Chem Phys 115:3497
123. Chattaraj PK, Chamorro E, Fuentealba P (1999) Chem Phys Lett 314:114